8
Reinforced and prestressed concrete using HPFRCC matrices

A. E. NAAMAN
University of Michigan, Ann Arbor, Michigan, USA
P. PARAMASIVAM
National University of Singapore, Singapore
G. BALAZS
Technical University of Budapest, Budapest, Hungary
Z.M. BAYASI
San Diego State University, San Diego, California, USA
J. EIBL
University of Karlsruhe, Karlsruhe, Germany
L. ERDELYI
Technical University of Budapest, Budapest, Hungary
N.M. HASSOUN
South Dakota State University, Brookings, South Dakota, USA
N. KRSTULOVIC-OPARA
Northeastern University, Boston, Massachusetts, USA
V.C. LI
University of Michigan, Ann Arbor, Michigan, USA
G. LOHRMANN
University of Karlsruhe, Karlsruhe, Germany

Abstract

A summary is presented of a number of representative studies on the use of HPFRCC in combination with conventional reinforced concrete and prestressed concrete. Examples of applications with reinforced concrete include the effect of fiber reinforcement on plastic rotation and ductility index; the use of fibers in the tensile zone area of reinforced concrete beams to control cracking and improve durability; the use of a SIMCON layer as reinforcement in a composite slab system; the use of SIMCON for repair and rehabilitation of reinforced concrete beams and columns; the use of fibers to improve shear resistance and replace shear reinforcement; the use of fibers to improve the seismic performance of reinforced concrete monolithic or cast-in-place framing joints subjected to cyclic loading; and the use of fibers to improve the impact resistance of reinforced concrete beams. Examples of applications with prestressed concrete include the reduction of transfer length of pretensioned strands due to fiber reinforcement, and the improved ductility of beams prestressed with fiber reinforced plastics reinforcements. A brief section on structural modeling is also provided.

Keywords: cracking, crack width, ductility, durability, end block, fiber concrete, impact, plastic hinge, prestressed concrete, reinforced concrete, repair, rehabilitation, shear, SIFCON, SIMCON, seismic performance, transfer length.

High Performance Fiber Reinforced Cement Composites 2. Edited by A.E. Naaman and H.W. Reinhardt.
Published in 1996 by E & FN Spon, 2–6 Boundary Row, London SE1 8HN, UK. ISBN 0 419 21180 2.

Contents

1 Introduction

1.1 Classes of Applications of HPFRCC

Applications of high performance fiber reinforced cement composites can be grouped according to the following (Fig. 1): 1) stand-alone applications in light structural elements such as cement boards, corrugated sheets, and roofing tiles, 2) selected zones of structures where their enhanced properties are needed, such as in the connection regions of seismic resistant frames (Fig. 2), 3) new structures or structural elements in combination with conventional reinforced and prestressed concrete, such as in super high rise buildings, and 4) in repair and rehabilitation work such as in bridge decks and piers. Fibers are added to reinforced or prestressed concrete structures for many reasons, among which to improve energy absorption, toughness, ductility, cracking, shear resistance, and durability (Fig. 3).

1.2 Some Background with Low End FRC Composites

The use of conventional fiber reinforced concrete in combination with reinforcing bars and prestressing tendons has been so far relatively limited in comparison to its use in stand-alone applications. Several studies have concluded of the beneficial effects of adding fibers to improve the flexural response, ductility, shear, torsion, and impact resistance of reinforced and prestressed concrete structures [3,7,8,10,11,24,28,36,39,53,58,66,69,71,72]. In most cases, a relatively low fiber content was used (steel fibers in less than 1.5% by volume), and the improvement due to fiber reinforcement was relatively small, suggesting difficult choices of trade-off between additional cost and improved performance. While the additional cost of fiber reinforcement may be given as the main reason for such slow progress, there is also evidence that the use of low end fiber reinforced concrete did not satisfy convincingly the expected performance. Examples include the early application of fiber reinforced

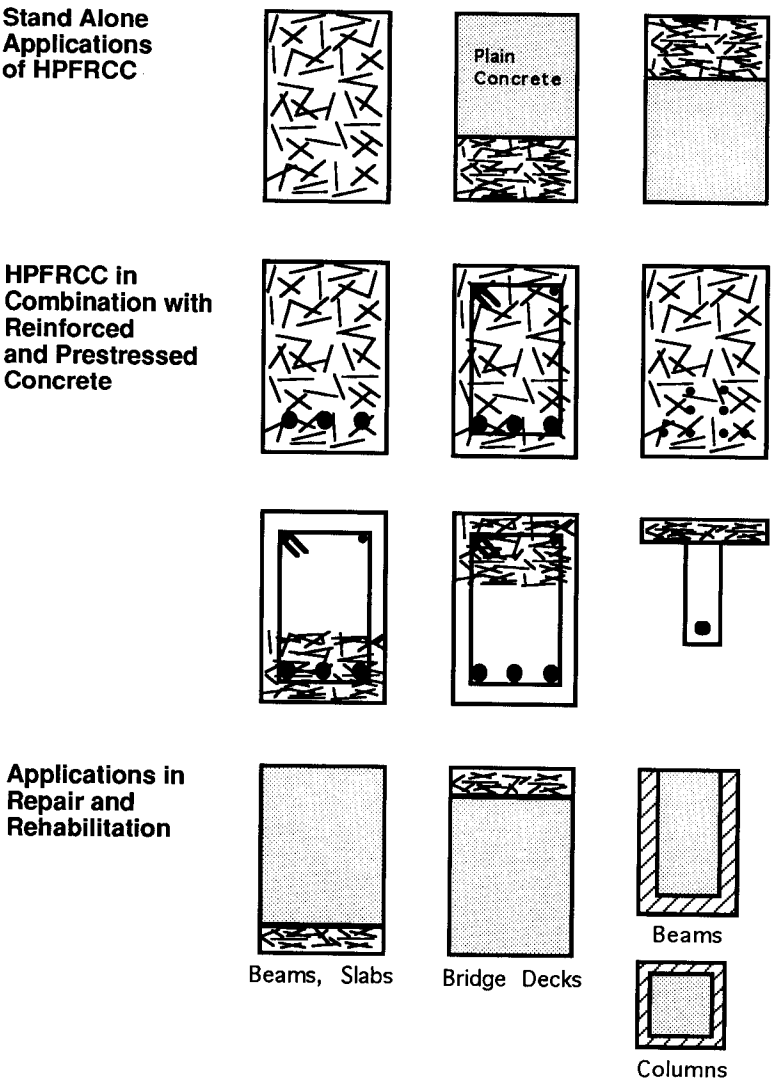

Fig. 1. Typical applications of high performance fiber reinforced cement composites.

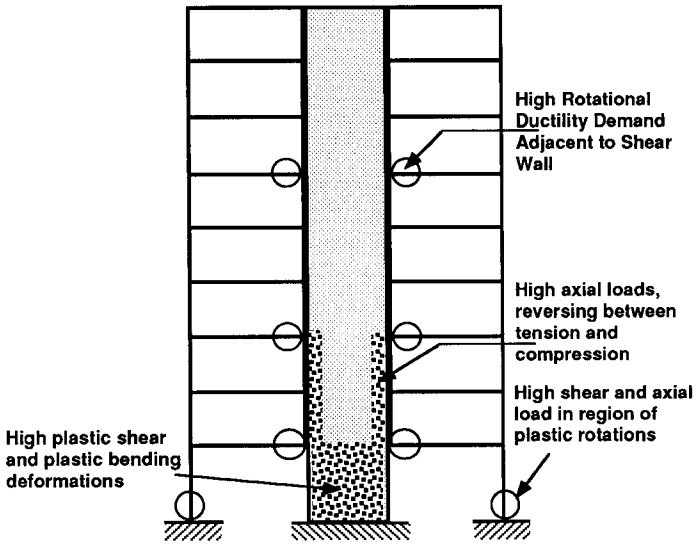

Fig. 2. Typical examples of selective use of HPFRCC in seismic resistant structures.

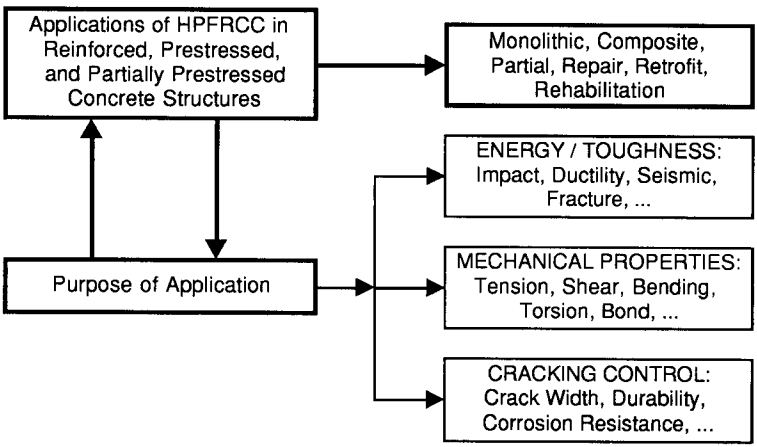

Fig. 3. Purpose of using HPFRCC in concrete structures.

concrete in the punching shear zones around columns in slab systems, and the beam-column connections in seismic frames [12,24,65]. However, high fiber content fiber reinforced concrete such as SIFCON was extensively used in military applications suggesting that there are cases where the use of HPFRCC is justified in spite of cost. It is believed that in order for fiber reinforced concrete to truly penetrate the reinforced and prestressed concrete market, it must provide significantly improved performance to the structure; the particular property of HPFRCC to develop multiple cracking and quasi-strain hardening behavior may indeed be the answer to such development.

1.3 Organization of this Chapter

This chapter provides a brief summary of a number of representative studies involving the use of HPFRCC in combination with conventional reinforced concrete and prestressed concrete. In some cases the fiber content is lower or just about equal to the critical fiber content; however the results can point to the possible beneficial effects, should the combination of fiber reinforcing parameters for HPFRCC be satisfied (see Chapter 1 in this volume). These studies are only representative; while they give an idea of what can be done, they do not necessarily cover all that can be done. Additional information on each investigation can be found in the references listed at the end of the Chapter.

Examples of applications with reinforced concrete include a study of the effect of fiber reinforcement on the length of the plastic hinge in the compression zone and the resulting ductility index; the use of fibers in the tensile zone area of reinforced concrete beams to control cracking and improve durability; the use of a SIMCON layer as reinforcement in a composite slab system; the use of SIMCON for repair and rehabilitation of reinforced concrete beams and columns; the use of fibers to improve the seismic performance of reinforced concrete monolithic or cast-in-place framing joints subjected to cylcic loading; and the use of fibers to improve the impact resistance of reinforced concrete beams; and modeling. Examples of applications with prestressed concrete include the reduction of transfer length of pretensioned strands due to fiber reinforcement, and the improved ductility of beams prestressed with fiber reinforced plastics (FRP) reinforcements. A brief section on structural modeling is also provided.

2 Crack Width Control in RC Beams

2.1 Introduction

Using micro-mechanical principles, Li and CO-workers at the University of Michigan have designed a family of high performance fiber reinforced cement composites which they call Engineered Cementitious Composites (ECC) [33,37,38].ECCs are very ductile short random fiber composites with good strain hardening and multiple cracking characteristics [32]. The specific ECC used in this application contain 2% by volume of polyethylene fibers (Spectra fibers by Allied Signal) with tensile strain capacity in excess of 5% and fracture energy of 27 kJ/m^2. The uniaxial tensile stress-strain curve of this composite is shown in Fig.4. The corresponding properties in regular concrete are approximately 0.05% and 0.1kJ/m^2.

2.2 Description and Scope

The durability of reinforced concrete (RC) members is often compromised by tensile cracking under flexural loads, followed by steel corrosion and concrete cover spalling. A new design for RC flexural members for the purpose of improving their durability was proposed [36]. The design makes use of an ECC layer to serve as the concrete cover. Two performance requirements are imposed on the ECC material to serve its intended purpose: (1) the ultimate tensile strain capacity of the ECC material should be greater than the maximum strain that can be developed in the outermost fiber at the tensile face of the R/C member, and (2) the crack width at the ultimate strain capacity of

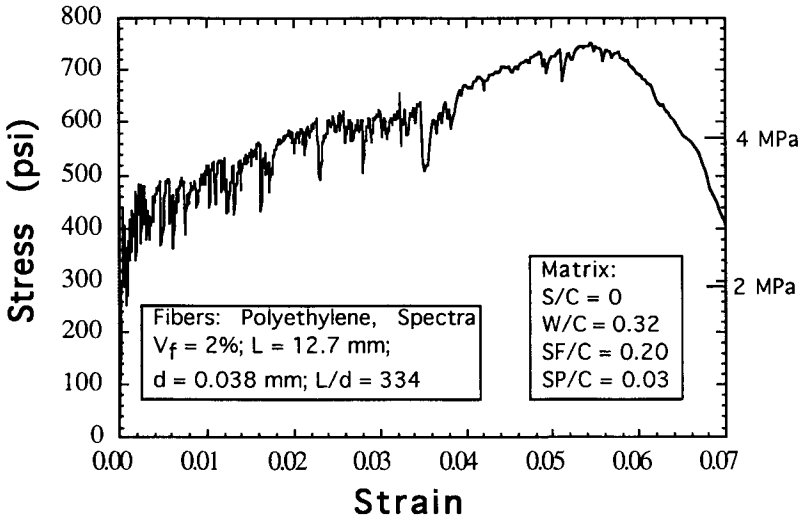

Fig. 4. Uniaxial tensile stress-strain curve of polyethylene ECC ($V_f = 2\%$)

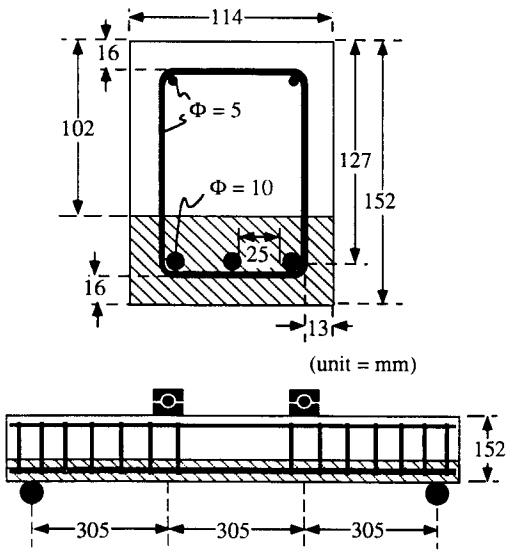

Fig. 5. Geometry of the reinforced concrete beam with ECC layer and reinforcement details.

the ECC material (hereafter referred to as ultimate crack width) should be less than the maximum crack width allowed in a particular environment. The first condition insures that no strain localization will take place in the ECC layer up to the peak load of the beam, and the second condition insures that the crack opening in the ECC is maintained below the allowable value. Assuming that at ultimate load, the strain in the extreme compression fiber of the concrete is equal to 0.003, and that plane sections remain plane, the strain in the extreme tension fiber of the ECC is found to be equal to 0.013. Therefore, the ECC that should be selected should have an ultimate strain capacity at least equal to 0.013. In addition, suppose that the member is to be exposed in an environment of sea water and sea water spray under wetting and drying. In this case, according to ACI Committee 224, the crack width should be limited to 0.15 mm. Therefore, the ultimate crack width of ECC should be less than 0.15 mm.

2.3 Experiments

A control RC beam and an otherwise identical RC beam with a layer of ECC substituted for the concrete that surrounds the main flexural reinforcement (Fig. 5) were tested under four point flexural loading. The main reinforcement consists of 3 No. 3 bars, corresponding to a reinforcement ratio ρ equal to 0.0147. Shear reinforcement was provided to insure flexural mode failure of the beam. Other specimen and loading configuration details can be found in [38]. For the purpose of this study, the ECC described earlier (Fig. 4) was selected as the material for the ECC layer. The average ultimate crack width for this material was measured to be 0.14 mm. Therefore, this material is expected to satisfy the performance requirements established for the ECC layer.

2.4 Results and Discussion

The crack patterns which develop in the control regular RC beam (Fig. 6a) and the ECC layered beam (Fig. 6b) were distinctly different. As the R/C beam with the ECC layer was loaded, the first crack could be seen above the ECC layer but difficult to see in the ECC layer. As the load was further increased, the cracks that developed in the concrete material diffused into many fine cracks when they met the ECC material.

Fig. 7 shows the moment curvature and crack width curvature diagrams for both beams. There is no significant difference between the moment curvature response of the two beams. However, the crack width-curvature response is significantly different. The crack width (width of first crack that appeared and monitored) in the control specimen increases almost linearly as a function of curvature. At peak load the width of the crack is approximately equal to 1.52 mm. If the beam is loaded 20 % beyond yield, the crack width in the beam reaches the ACI crack width limit for interior exposure (0.40 mm). Any cracks of width larger than this limit may result in a high rate of reinforcement corrosion. Overload of a properly designed member (satisfying crack width criteria under service load) can drive cracks significantly wider resulting in eventual durability problems. Fig. 7 shows that for a given curvature the crack width measured on the beam with the ECC layer is much smaller than that measured on the control R/C beam. At ultimate load the crack width reaches 0.19 mm. Also the strain measured in the ECC material at the bottom of the beam was 0.026 which is smaller than the ultimate strain capacity of the material.

Based on the above results and a study of water flow through cracked concrete by Tsukamoto [65] one could conclude that the flow of aggressive substance into a RC member could be significantly reduced, if not brought down to zero. Tsukamoto's study suggested that the critical crack width below which no flow occurs for an FRC is about 0.1 mm. Under service load conditions (about 60% of ultimate) the crack width in the RC beam with the ECC layer is limited to 0.05 mm. Therefore, it can be concluded that under service load conditions the ECC layer will prevent the migration of any aggressive substance (through water) into the concrete or the reinforcement. Since above the critical crack width, the flow rate scales with the third power of the crack

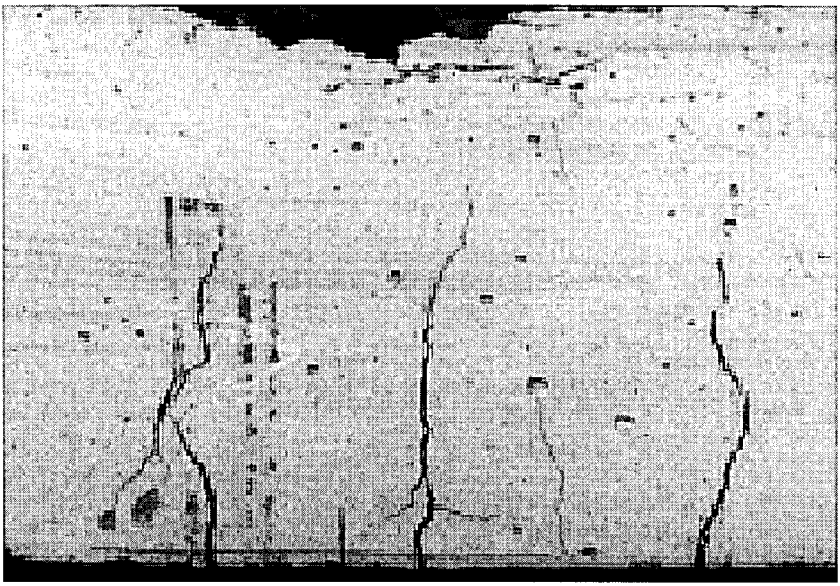

(a)

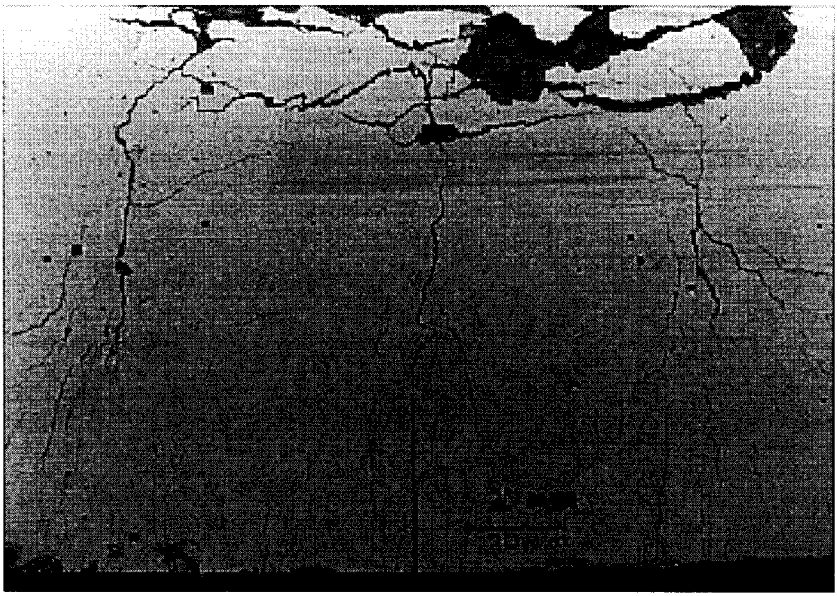

(b)

Fig. 6. Crack pattern: a) control RC beam; b) RC beam with ECC layer.

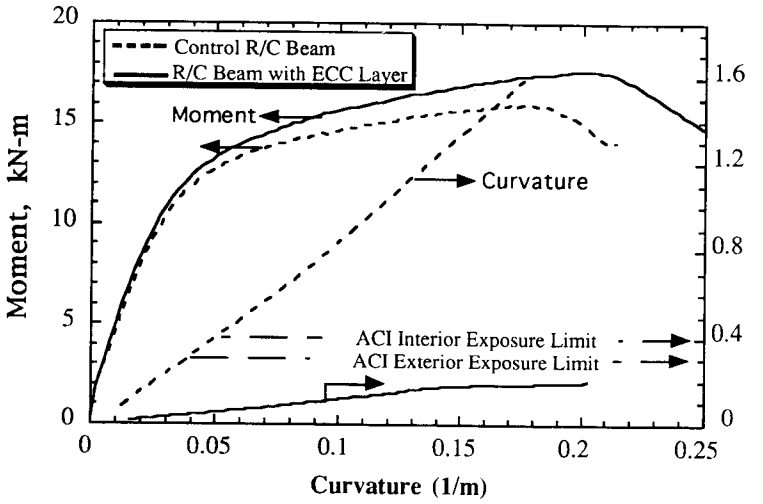

Fig. 7. Moment and crack width versus curvature diagrams. (1kip-in. = 0.113 kN-m; 1 in. = 25.4 mm)

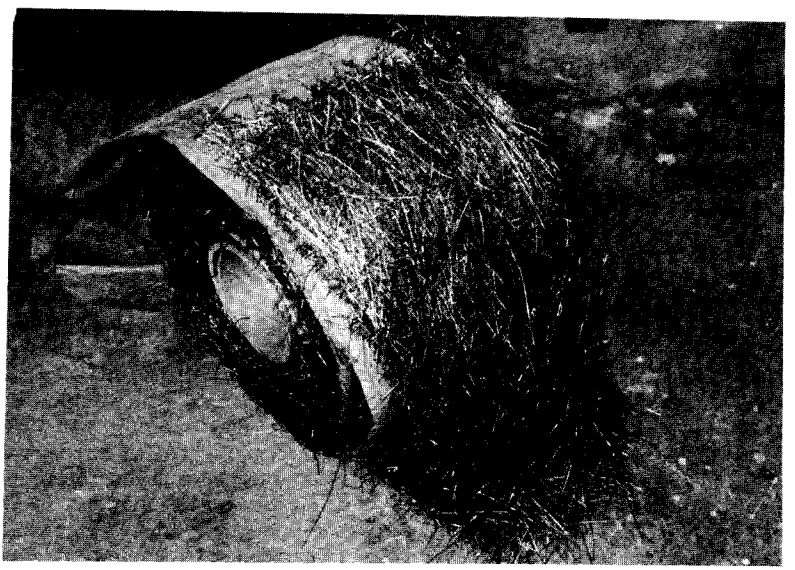

Fig. 8. SIMCON roll as delivered to the laboratory or construction site.

width, a small reduction in the crack width translates into a significant reduction in the flow rate.

3 Composite Slabs using Slurry Infiltrated Mat Concrete - SIMCON

3.1 Experimental Program

An experimental investigation by Bayasi at San Diego State University was targeted towards investigating the properties of composite slabs made from an HPFRCC tensile deck and a plain concrete topping [13,14]. The proposed system is intended as an alternative to the current system of composite steel deck - concrete topping used for floor slabs [56]. Slurry infiltrated mat concrete (SIMCON) was the candidate HPFRCC to replace the steel deck. SIMCON was shown to have superior flexural/tensile properties [25].

Six composite concrete slabs were constructed. They consisted of a bottom layer (deck) of slurry infiltrated mat concrete (SIMCON) and a top layer (topping) of conventional concrete. Composite slab dimensions were 5.25 in x 14 in x 3 ft (13 x 36 x 91 cm). Fig. 8 shows a typical SIMCON roll as delivered to the laboratory. The SIMCON roll is made out of fibers of rectangular sections of dimensions of 0.005 x 0.1 x 5.6 in (0.13 x 2.5 x 142 mm) resulting in an aspect ratio of 220. The roll was cut to dimensions, placed in the mold, and infiltrated by a cement slurry to form a bottom reinforcing layer or deck of slab. The cement slurry had a water/cement ratio of 0.32, sand/cement ratio of 0.50 and superplasticizer/cement ratio of 1%. The top surface of SIMCON was left unfinished with fibers protruding so that adequate bond to the concrete topping would develop. The flow of slurry mix used for SIMCON was 100%. External vibration was used for consolidation and to facilitate penetration of the cement slurry into the fiber mats. Following pouring, the SIMCON specimens were kept in their molds covered with plastic sheeting for 24 hours prior to demolding. They were then cured under 100% RH and 72°F (21°C) until an age of 7 days. Thickness and volume fractions of steel fibers in the SIMCON deck layers are given in Table 1; average tensile strength and modulus of rupture for typical SIMCON specimens are given in Table 2. Note that Table 2 provides information on the nominal flexural strength of SIMCON deck in composite slabs as well as the flexural and direct tensile strengths of the SIMCON layer tested separately [13]. The tensile strength was obtained from direct tensile tests on dog-bone specimens.

Following curing of the SIMCON layer, the plain concrete topping was placed so that the total thickness of each composite slab is 5.25 in (135 mm). The concrete topping mix consisted of a water/cement ratio of 0.50, aggregate/cement ratio of 5.0, crushed rock/total aggregate ratio of 0.60, maximum aggregate size of 3/4 in (19 mm) and superplasticizer/cement ratio of 0.6%. Slump for the concrete topping mix was 4 in (100 mm). External vibration through a vibrating table was used in preparing the composite slab specimens. Each composite slab was cured for 7 days under the same conditions used for the SIMCON deck layers. Testing of composite slabs was undertaken at an age of 28 days of the concrete topping (age of 35 days for the SIMCON decks). Testing was in 4-point loading over a span of 30 in (76 cm), using a servo-controlled testing machine. A special yoke was utilized to determine the value of net deflection (Fig. 9). Deflections were measured via two displacement transducers mounted on the specimen. The average load-deflection curve of each specimen was obtained via an electronic recorder linked to the displacement transducers.

3.2 Data Analysis and Test Results

The nominal stress (i.e. the equivalent elastic bending stress) vs. deflection curves for composite SIMCON deck-concrete topping slabs are shown in Fig. 10. It can be

Table 1. Thickness of SIMCON layers and fiber content by volume

Specimen No.	SIMCON Deck Thickness in (mm)	Steel Fiber Volume (%)
1 & 2	2.15 (55)	4.75
3 & 4	1.75 (45)	3.00
5 & 6	1.35 (35)	3.75

Table 2. Typical properties of SIMCON and composite slab

Fiber Volume	Composite Flexural Strength, psi(MPa)	SIMCON Flexural Strength, psi(MPa)	SIMCON Tensile Strength, psi(MPa)
4.75 %	1,790(12.4)	3,340(23.1)	930(6.4)
3.75 %	1,480(10.2)	3,130(21.6)	870(6.0)
3.00 %	1,220(8.4)	2,870(19.8)	680(4.7)

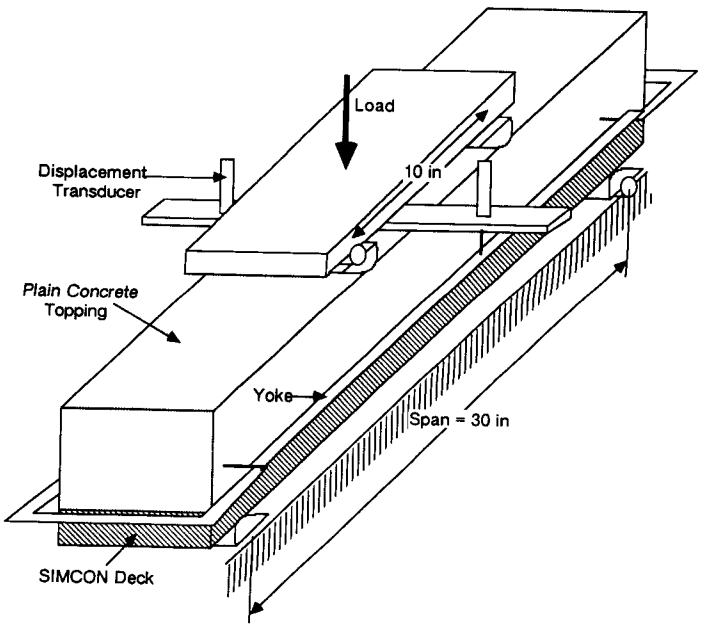

Fig. 9. Testing set-up used for composite slabs.

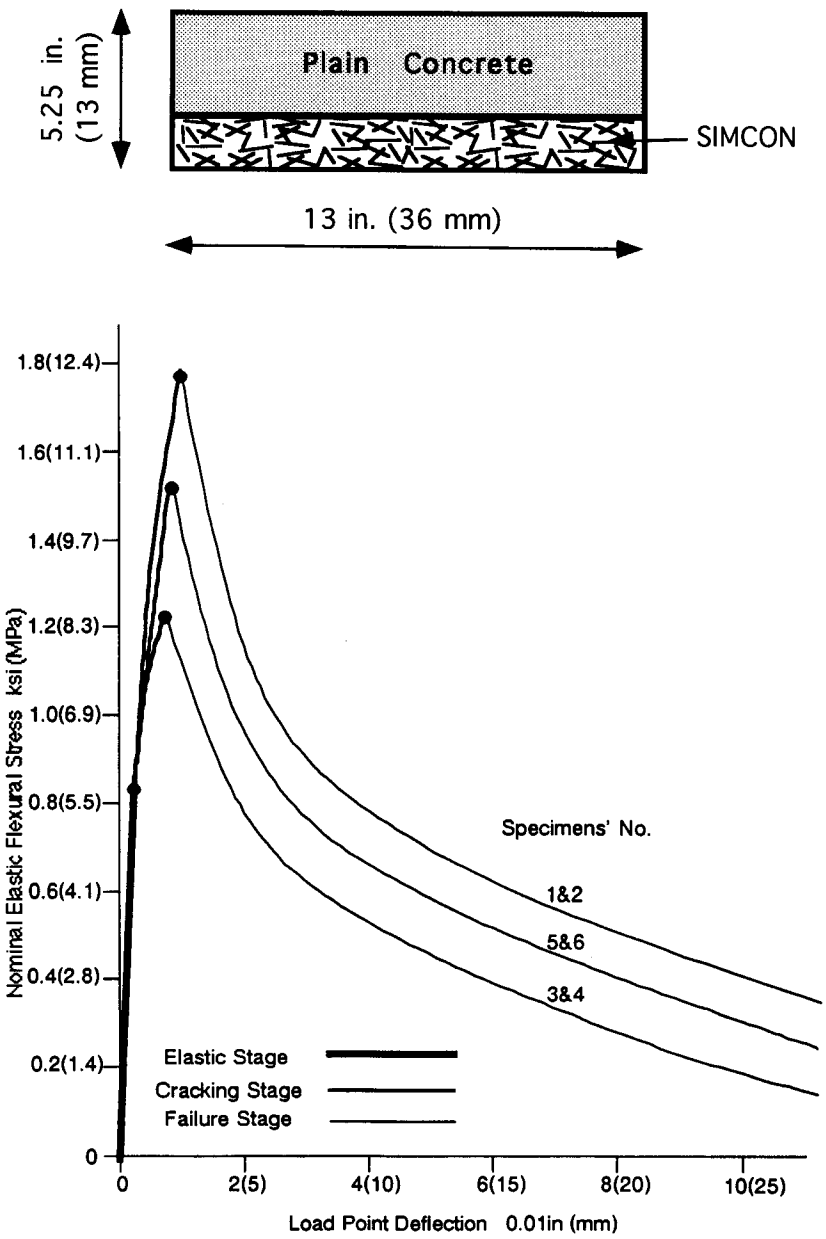

Fig. 10. Observed flexural stress-deflection curves of composite slabs using a SIMCON tensile layer.

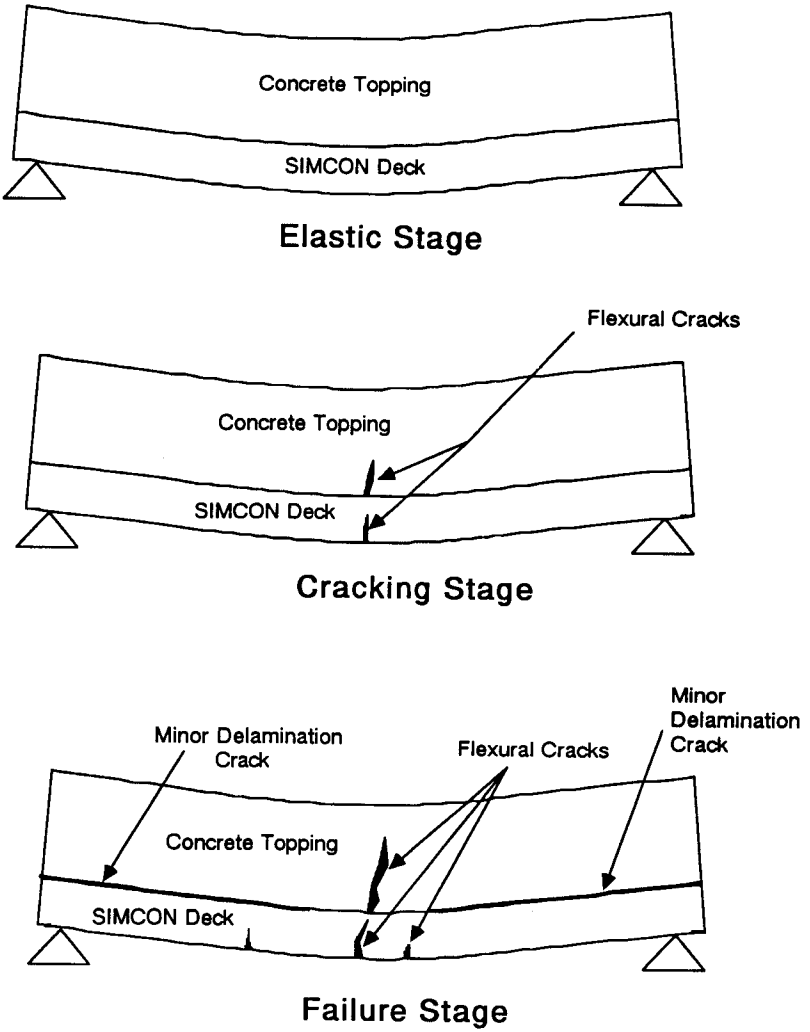

Fig. 11. Flexural behavior of composite slabs with SIMCON tensile layer.

observed that the flexural strength increases as the volume fraction of fibers in SIMCON increases. Differences between specimens 2-4 and 5-6 also indicate that for the same total volume of fibers, it is better to use a thin reinforcing layer rather than a thick one.

The behavior under loading starts with an initial elastic stage followed by flexural cracking of SIMCON and concrete. The second stage of behavior can be described as strain hardening where the load increases, more cracks appear, crack widths increase, and stiffness decreases. Furthermore, minor delamination cracks also developed at the interface between the SIMCON layer and the concrete topping. The third and final stage is the failure and softening stage. Generally failure of composite slabs started with a major tension/flexural crack through the SIMCON deck and concrete topping. Fig. 11 schematically illustrates the various stages of flexural behavior.

3.3 Conclusion

The preliminary test results presented herein indicate that composite SIMCON deck-concrete topping slab can be considered an alternative method for slab construction. The SIMCON deck layer can be precast, transported and used at the site as formwork as well as reinforcement for the composite slab. This proposed system may be considered as a substitute for the current composite steel deck concrete slab system. However some additional research is needed to better understand the interaction of the SIMCON deck layer and the concrete topping and to insure a strong and ductile interfacial zone between them.

4 Repair and Rehabilitation using Slurry Infiltrated Mat Concrete - SIMCON

4.1 Introduction

As part of an NSF Earthquake Hazard Mitigation Project on "Repair and Rehabilitation of Non-Ductile R.C. Frames Using High Performance Fiber Reinforced Cement Composites," Krstulovic-Opara and Uang [31] are investigating the behavior of composite structural elements made of conventional reinforced concrete combined with a novel HPFRCC called Slurry Infiltrated Mat Concrete (SIMCON). SIMCON (Fig. 8) is made by infiltrating continuous steel fiber-mats, with a specially designed cement-based slurry. An important advantage of continuous fiber-mats is the increased fiber length and fiber aspect ratio, which lowers the critical fiber volume fraction necessary to achieve strain hardening, and substantially increases strength, toughness and spall resistance. SIMCON thus reaches tensile strengths of up to 17 MPa at strains of up to 1.5% with only 5.29% fiber volume fraction. Distribution and orientation of fibers within fiber-mats can also be more accurately controlled, which further increases fiber efficiency. Finally, continuous fiber-mats, which are conveniently delivered in large rolls, can be easily installed by wrapping around or laying over existing reinforced concrete elements. SIMCON is thus well suited for both durability and structural repair/retrofit, as well as new construction of high performance structural elements. Typical tensile and bending properties of SIMCON are given in Section 3, Tables 1 and 2, of this Chapter.

4.2 Experimental Investigation

To develop a SIMCON based procedure for seismic retrofit of non-seismically designed beam-column sub-assemblages, Krstulovic-Opara et al. [32], investigated the behavior of composite beam elements made of conventional reinforced concrete in combination with SIMCON, as shown in Figure 1 a. All beams were designed following ACI 318-89, to exhibit a ductile flexural failure. Reinforcement ratio in both tension and compression were 1.48 %, with the balanced reinforcement ratio being 5.65 %. Fiber volume fraction of SIMCON used in this investigation was 5.25%. Beams were tested

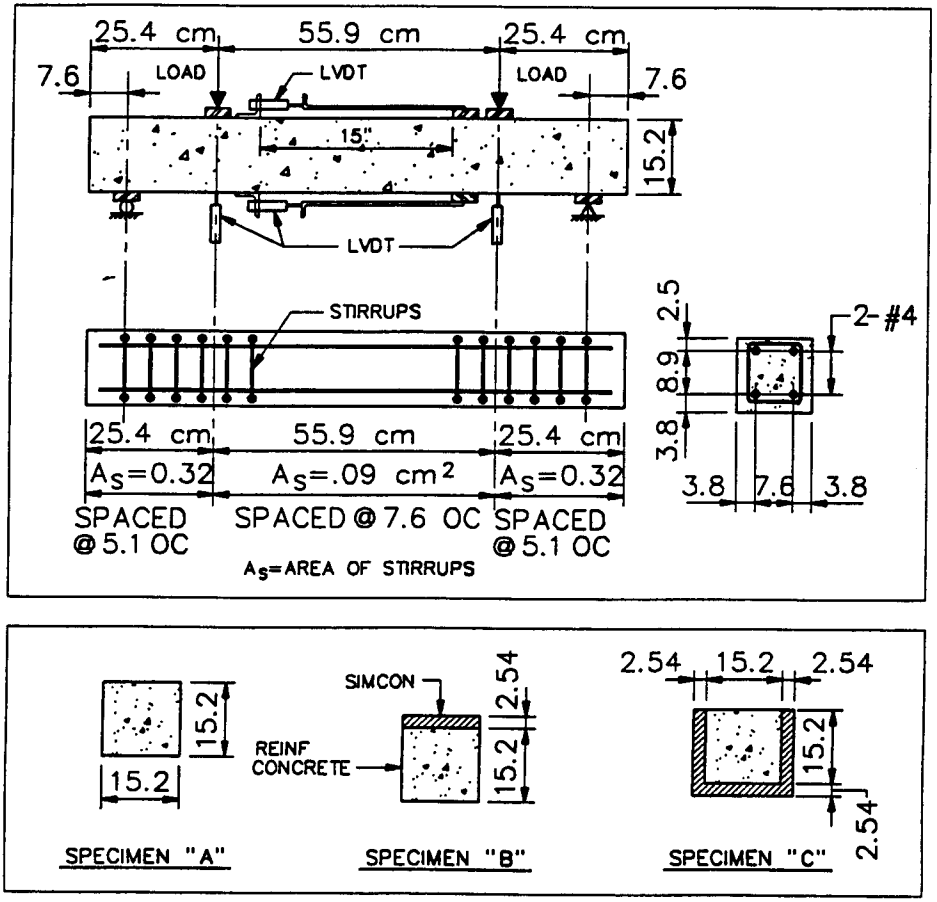

Fig. 12. Layout of the reinforced beams tested using SIMCON.

in four point bending, as shown in Figure 12. The curvature in the midspan portion of the beam was measured using two LVDTs placed along the top and bottom fibers.

4.3 Analytical Modeling

Parallel to experimental investigation, an iterative non-linear analytical procedure was developed for predicting a full range of the moment-curvature behavior [3]. The procedure was developed based on the previous work by Naaman et al. [49] and assuming full bond between reinforcing bars, concrete, and SIMCON. Behavior of concrete in compression was represented using the standard model developed by Kent and Park [26], while the behavior of reinforcing steel in both compression and tension was defined using the model developed by Sargin [62]. Behavior of SIMCON in compression was represented using the model developed for SIFCON by Naaman et al. [2,43], while the behavior in tension was modeled as [30]:

$$\sigma = \sigma_{cu}\left[1 - \left(1 - \frac{\varepsilon}{\varepsilon_{cu}}\right)^{A}\right] \quad \text{for } \sigma \le \sigma_{cu} \tag{8.1}$$

$$\sigma = \sigma_{cu}\left[1 - (13 - 2\ V_f)\frac{2\,\delta}{L}\right]^{5} \quad \text{for } \sigma > \sigma_{cu} \tag{8.2}$$

$$A = \sqrt{E_c \frac{\varepsilon_{cu}}{\sigma_{cu}}} \tag{8.3}$$

where σ_{cu} is the ultimate composite tensile strength, ε_{cu} is the strain at the ultimate strength, E_c is the composite elastic modulus, δ is the width of the crack opening, V_f is the fiber volume fraction in percent, and L is the fiber length. Note that Eq.8.2 is valid only for the range of fiber volume fractions of mats currently available on the market, i.e., volume fractions less than 6%. It should be also noted that the descending branch, defined by Eq. 8.2, reaches zero value before the critical crack opening displacement reaches the value of L / 2. This is contrary to the behavior observed in short fiber HPFRCs, such as SIFCON. However, such behavior can be explained because of partial fiber rupture before the complete pull-out of long fibers takes place.

After defining the section geometry and material models, the section is subdivided into a series of a very thin layers (e.g., 100 layers). The iteration procedure is then started by first assuming: (1) strain at the top fiber, and (2) depth of the neutral axis. The compressive or tensile forces of each layer are then calculated. At the end of calculation the total compressive force, C, is compared to the total tensile force, T. If forces are in equilibrium, the next step is started in which moment is calculated. Otherwise the assumed strain distribution is adjusted, and the whole iterative procedure is repeated. The resulting moment and assumed curvature are then saved and the calculation is repeated for a larger curvature. This way a complete moment - curvature relationship is obtained. Predicted analytical moment-curvature curves are compared to the experimentally obtained values in Figure 13. A very good correlation is observed.

4.4 Conclusions

Based on the observed experimental and analytical investigation it was concluded that SIMCON can successfully interact with conventional reinforced concrete elements, substantially increasing both load and energy-absorption capacities. Adding a layer of SIMCON in the compression zone and/or tension zone increases both the lever arm and strength of the compression and tension zones, respectively. This leads to a significant increase in strength and energy absorption capacity of the beam.

In the case of specimens investigated in this particular research [29,30] both flexural capacity and energy absorption up to the maximum moment exhibited an increase of 2.2 and 1.9 times the reference values, respectively. Furthermore, observable cracking started only at 80% of the flexural strength, while maximum crack widths were well

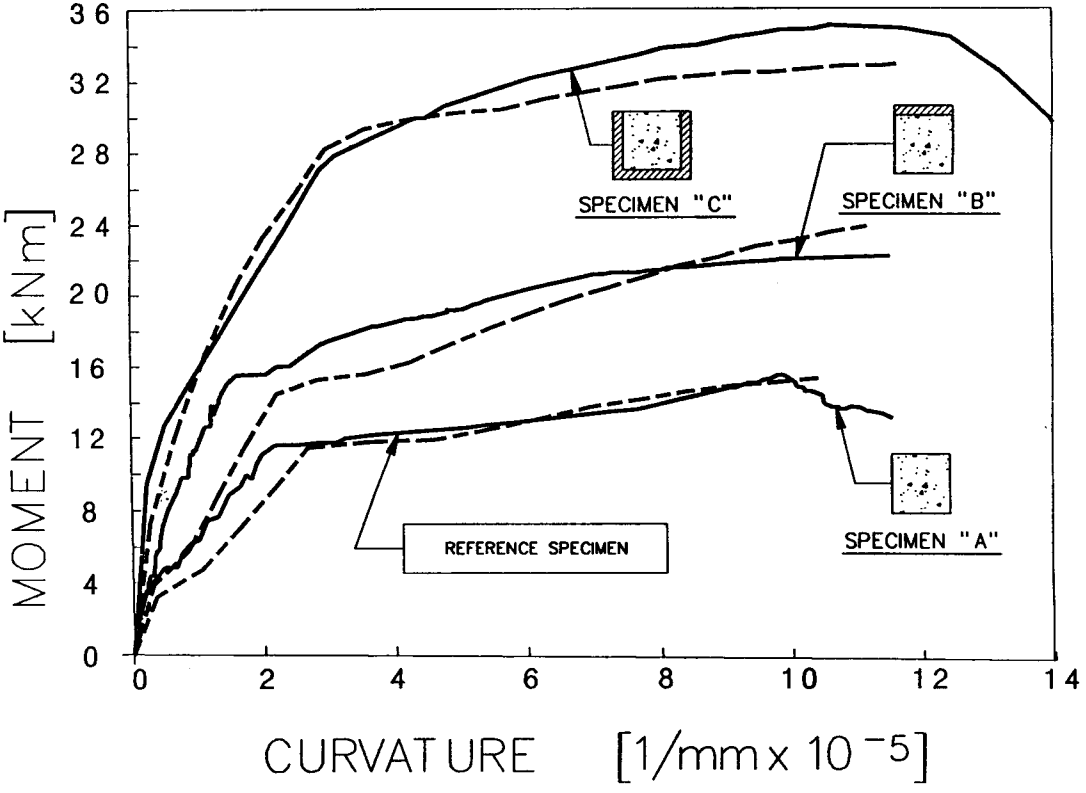

Fig 13. Comparison between experimentally observed and analytically predicted moment curvature behavior (letters A, B and C refer to the specimen types defined in Fig. 12).

within the crack size limits of 0.2 mm (0.0078 in.) required by ACI standards for reinforced concrete elements exposed to severe environments [5].

The construction of a SIMCON-based retrofit was much simpler than similar retrofit solutions using short fiber FRCs, reinforced concrete, steel plates or different non-cement based fiber composites. It is thus anticipated that the proposed technique is less labor- and equipment-intensive and more economical than conventional jacketing methods. It uses widely available construction equipment and building expertise, and can thus be easily introduced to the field without major re-training and changes in existing construction practices.

5 Plastic Hinge in RC Beam-Column Joint

5.1 Performance Criteria

In earthquake resistant design, the structural system performance requirements can be specified in terms of minimum ductility ratio, number of load cycles, sequence of application of load cycles and residual strength at the end of loading. On the beam-column connection component level, the following performance criteria are desirable: (i) ductile plastic hinge behavior under high shear stress, (ii) no congestion of transverse reinforcement for confinement and for shear, (iii) maintaining concrete integrity under load reversals, and (iv) concrete damage contained within a relatively short hinging zone. These performance criteria are difficult to achieve with ordinary concrete, although some encouraging results have been obtained with fiber reinforced concrete. Desirable performance of the plastic hinge is difficult to translate directly into numerical quantities of materials property requirement. In general, however, it may be expected that the following properties of the concrete material in the plastic hinge should be advantageous:

a. high compression strain capacity to avoid loss of integrity by crushing,
b. low tensile first cracking strength to initiate damage within the plastic hinge,
c. high shear and spall resistance to avoid loss of integrity by diagonal fractures,
d. enhanced mechanisms that increase inelastic energy dissipation.

5.2 R/C Beam-Column Connection

Mishra and Li investigated the use of a strain-hardening ECC to achieve a ductile connection through fiber reinforcement instead of additional stirrup confinement [38]. ECC is defined in Section 2 of this Chapter. The sub-assemblage of RC moment resisting frame selected for the testing program is shown schematically in Fig. 14. The test specimen represents two half beams connected to a stub column, in a strong column-weak beam configuration. The beams are simply supported at their ends to represent mid-span inflection points, under lateral loading of a framed structure.

Two specimens, one using plain concrete for the entire specimen and the other using ECC material in the plastic hinge zone and plain concrete in the rest of the specimen, were tested. The concrete mix proportions for the first specimen were as follows: S/C = 1.72, CA/C = 1.72, W/C = 0.45, where C, S, CA, and W stand for cement, sand, coarse aggregate, and water respectively. The ECC material used for the second specimen had the following mix proportions (Fig. 4): S/C = 0.5, CA/C = 0., W/C = 0.32, and SF/C = 0.2, SP/C = 0.03, where SF stands for silica fume and SP for superplasticizer. Ordinary reinforcement detailing (Fig. 14) was used for both specimens to highlight the contribution of the ECC. Equal tension and compression steel ($\rho = 0.017$) was provided in form of two #6 bars each at the top and bottom of the section. Closed stirrups (#2 bars) were provided at 4 in. (100 mm) spacing throughout the span. The shear span of the specimen was 30 in. (0.75 m) and effective depth was 8.63 in. (0.22 m), leading to a shear span to depth ratio of 3.5. The loading history

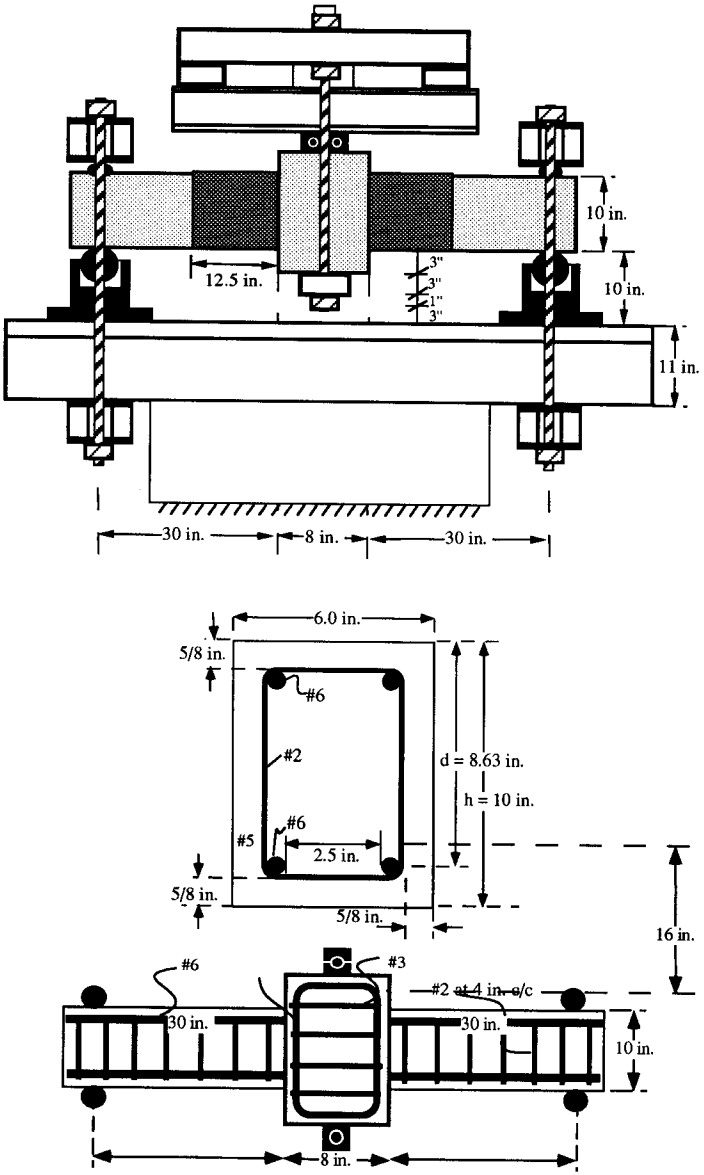

Fig. 14. Experimental set-up and reinforcement layout (1 in. = 25.4 mm).

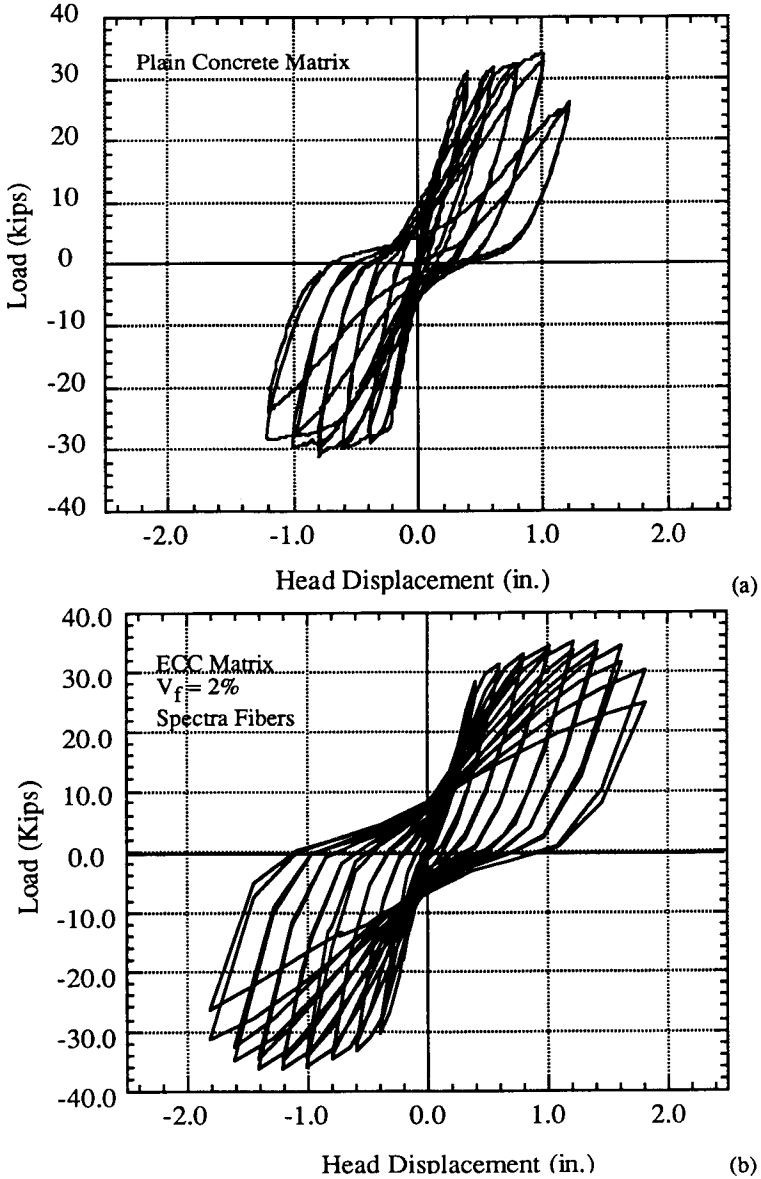

Fig. 15. Load-deflection hysteretic response for: a) specimen # 1 with plain concrete plastic hinge, and b) specimen # 2 with ECC plastic hinge. (1 kip = 4450 N; 1 in. = 25.4 mm)

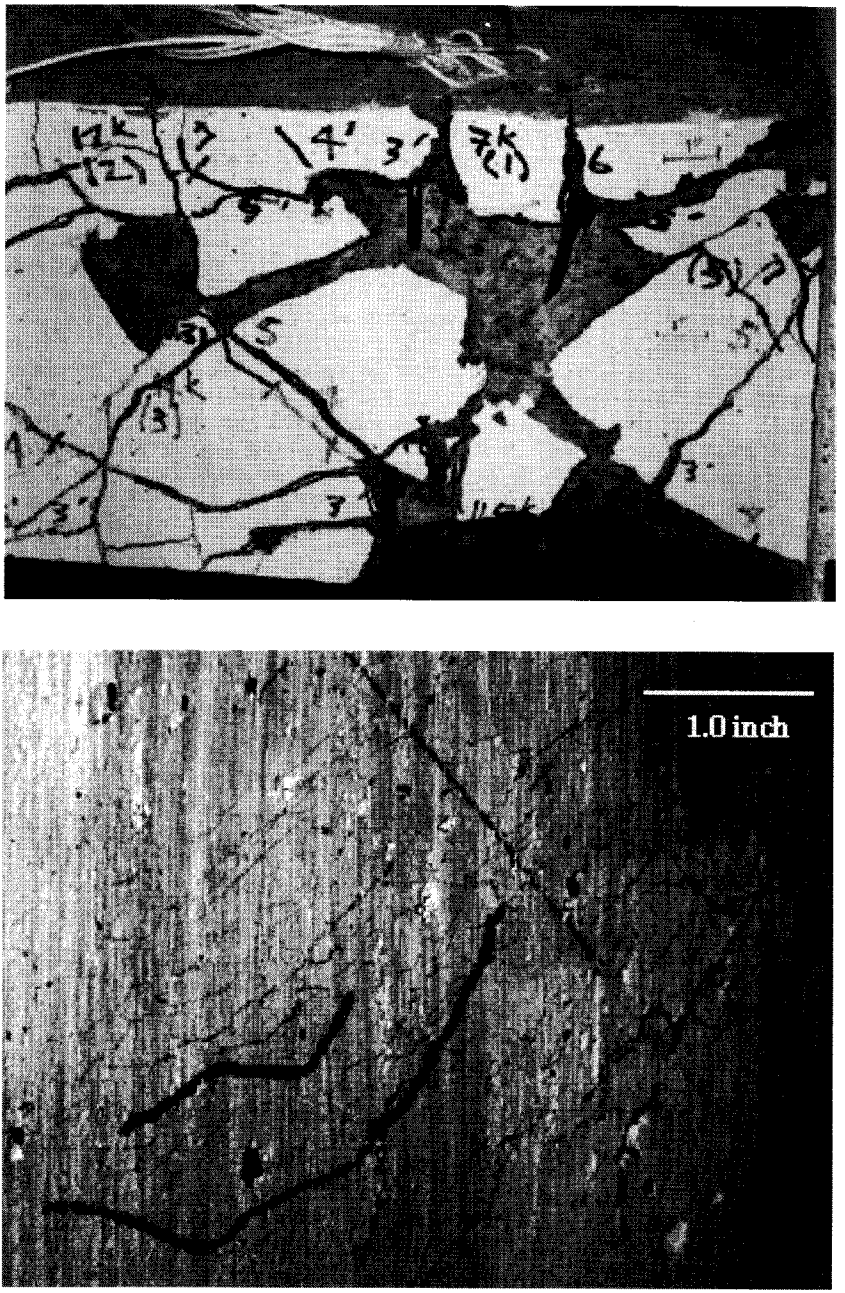

Fig. 16. Photograph of final failure in the plastic hinge zone of: a) control specimen, and b) specimen with ECC layer.

used in this testing program consists of simple multiple steps of symmetric cycles of increasing displacement amplitude [37].

5.3 Results and discussions

The load vs. deflection hysteretic behavior is shown in Figure 15. For the plain concrete hinge, the displacement ductility factor defined as the ratio of ultimate deflection (corresponding to a failure load that is about 20% lower than the maximum load carrying capacity) to yield deflection, was about 4.8. For the ECC hinge, the displacement ductility factor increased to 6.4, with less amount of pinching and a much reduced rate of stiffness degradation. The cracking pattern (Fig. 16) was distinctly different with more cracking taking place in the plastic hinge zone with ECC than in the zone outside as in the case of the plain concrete control specimen. The damage was mostly in the form of diagonal multiple cracking in perpendicular direction. Unlike the control specimen which failed in a predominantly shear diagonal fracture, the ECC specimen failed by a vertical flexural crack at the interface between ECC plastic hinge zone and the plain concrete at the column face. No spalling was observed in the ECC hinge, whereas the concrete cover mostly disintegrated in the control. The cumulative energy over the load cycles up to failure for the two specimens showed that the ECC hinge absorbed about 2.8 times as much energy as the control. While the control specimen behaved similarly to the ECC hinge specimen in its range of deflection, the ECC specimen outperformed the control specimen in the deflection regime beyond 1.2 in. (30 mm).

5.4 Conclusions

The study presented in this section demonstrates that the high performance ECC can be utilized in structural applications to enhance structural performance. Since the ECC uses two volume percent of synthetic fibers in chopped form, there is no processing difficulty. The specimens have been manufactured by regular casting method and using ordinary laboratory mixers. Further tailoring of the ECC, with the aid of the micro-mechanical models, is possible to reduce the amount of fibers and hence the cost.

6 Seismic Joints for Precast Concrete Frames

6.1 Description of Framing System and Test Program

The main goal of this research is to contribute to the development of a high energy absorbing joint (or joints) for precast concrete structures in seismic zones [52,63,64]. The structural framing system is described in Fig. 17. The frames are made of: 1) precast (or precast prestressed) concrete columns possibly several stories high, with corbels or short beam extensions extending about one beam depth from the face of the column, 2) precast (or precast-prestressed) beams connected to the extended columns, 3) a special cast-in-place (CIP) reinforced concrete joint connecting the columns corbels to the beams.

The matrix of the joint is made from high performance fiber reinforced cement composites (HPFRCC) such as high fiber content fiber reinforced concrete and SIFCON (Slurry Infiltrated Fiber Concrete). Matrices used in SIFCON have very fine particles composition to produce a slurry paste. The joint is designed to act as an energy dissipating connector between the beam and the column elements. The use of high fiber content in the matrix of the joint is meant to insure high ductility, increased energy absorption, reduced spalling, and superior shear resistance during load reversals.

This investigation is still ongoing at the time of this writing; the main overall objective of the research is to understand the fundamental mechanisms that control the properties of the joint and its response under monotonic and cyclic loads.

For one test series completed so far, the cast-in-place matrix was slurry infiltrated fiber concrete (SIFCON) and, for the other series, the matrix was conventional fiber reinforced mortar of concrete with high fiber content (up to 4% by volume). More than

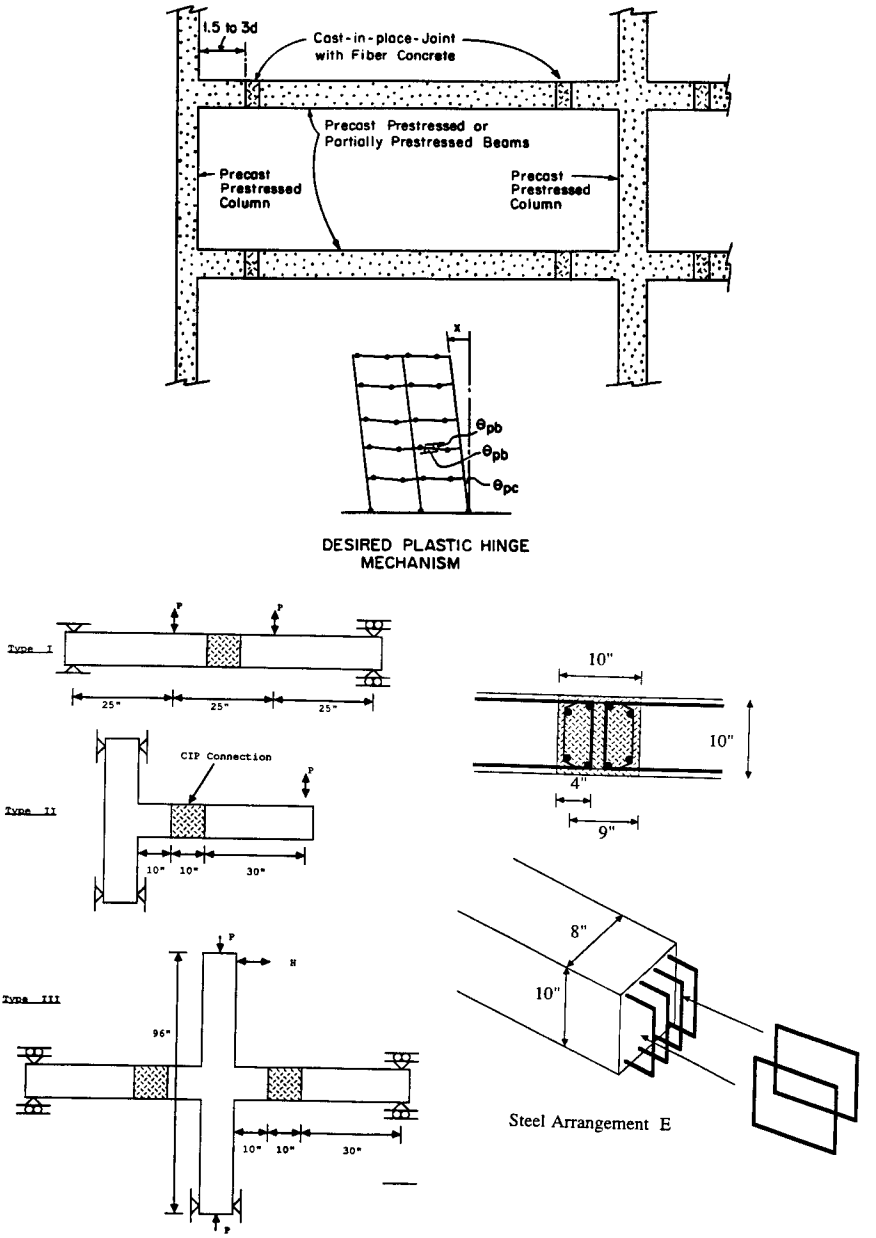

Fig. 17. Typical framing system for HPFRCC cast-in-place joints (1 in. = 25.4 mm; 1 ft. = 30.5 cm.).

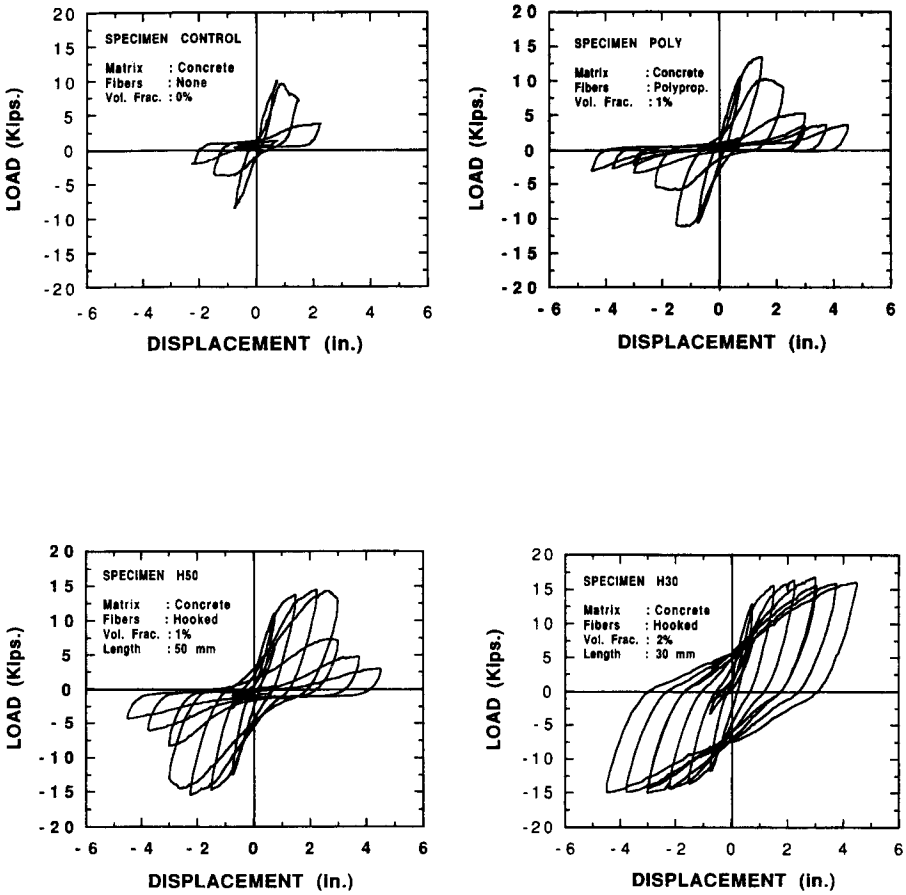

Fig. 18. Typical hysteretic load-displacement response curves of beam column subassemblages with HPFRCC cast-in-place joints. (1 in. = 25.4 mm; 1 kip = 1000 lbs = 4.45 kN)

twenty specimens were tested, including beam type specimens and beam to column subassemblages (typical interior and typical exterior). Typical load-displacement hysteresis response curves are shown in Fig. 18 and compared to the control specimen containing a matrix without fibers [64,69].

6.2 Main Results

Based on the results so far obtained, the following observations were made demonstrating the superior performance of the HPFRCC joint in comparison to the joint where plain concrete was used.

1. At failure, more distributed cracking was observed inside the CIP joint with HPFRCC; the damage was spread over a larger area than for the control joint with plain concrete matrix;

2. The load-displacement hysteretic response was a fuller curve for the HPFRCC joint, maintaining at least 80% of first cycle maximum load, at two to three times the number of cycles achieved by the control;

3. The displacement ductility of the HPFRCC joint was up to six times that of the control;

4. The cumulative energy dissipation of the HPFRCC joint was 4 to 13 times that of the control joint without fibers.

5. The HPFRCC joint showed substantially slower stiffness degradation than the control joint, at each loading cycle;

In conclusion, there is no doubt that the use of HPFRCC in seismic resistant structures is bound to increase, as evidenced from the enormous benefits they can contribute to the behavior of the structure and the resulting safety to the public.

7 Plastic Rotation and Ductility Index

7.1 Experimental Program

A research investigation was conducted by Hassoun [73] at South Dakota State University with the aim of studying the physical properties, ductility index, inelastic behavior and plastic rotation capacity of fibrous reinforced concrete continuous beams loaded to failure. The study presents the variation of the above parameters as they are affected by using different percentage combinations of steel fibers and main steel reinforcement based on the concept of limit state design of hyperstatic concrete structures. In such structures, sufficient ductility and rotation capacity are required after the steel yields, to develop plastic hinges at all critical sections, so that a mechanism is reached. Some background information can be found in [16,17,18,19,54].

For this purpose, eighteen two-span beams were cast and tested to failure. The beams were identical in dimensions, had a total depth of 8 in. (200mm), a width of 5 in. (125 mm) and a total length of 11 ft. (3.35m). The beams were divided into six groups. The first three groups G1, G2 and G3, were designed as singly reinforced with three different main reinforcement ratios, 0.67%, 1.21% and 1.89%. Each group with a specific main reinforcement, say 0.67%, consisted of three beams that contained three different steel fibers ratios: 0%, 0.8% and 1.2%, with a total number of 9 beams. The second three groups, G4, G5 and G6 contained compression reinforcement in addition to the main tension reinforcement. The percent of compression reinforcement (A'_s/bd) when used was 0.7% in all cases. Also, each group consisted of three beams that contained 0%, 0.8% and 1.2% steel fibers by volume of concrete. All beams were

made of normal weight concrete with a standard cylinder strength of about 5000 psi (35 MPa), (The range was between 4800 and 5275 psi). Grade 60 steel according to ASTM 615 was sued in all beams. The hooked end steel fibers used in this research program had an aspect ratio of 100 with a length of 50 mm and a diameter of 0.5 mm. Strain gages were placed at different locations on steel bars and concrete. The beams were tested under two concentrated loads, one at the center of each span (Fig. 19). Proper arrangements of the main steel reinforcement in the positive and negative moment areas were made, and adequate shear reinforcement was provided.

7.2 Presentation and Discussion of Test Results

a. Plastic Hinge Length HL

The length of the plastic hinge on each beam was measured as the distance between the extreme cracks on each side of the support. Based on the test results from all beams, the plastic hinge length can be evaluated as follows:

$$HL = (1.06 + 0.13\ \rho V_f)d \qquad (8.4)$$

where ρ is the tensile reinforcement ratio in percent, V_f is the volume fraction of fibers in percent, and d is the effective depth of the concrete beam. Figure 20 shows half the plastic hinge length measured to the center of the middle support.

b. Curvature Distribution Factor ß

The curvature along the plastic hinge length varies between a maximum at the middle of the plastic hinge to almost zero at the end of plastic length (Fig. 20). The average curvature along HL is equal to ß times the plastic rotation Φ_p. From the test results, β can be evaluated as follows in terms of the fiber content:

$$ß = (0.56 - 0.16\ V_f) \quad \text{where } 0 \le V_f \le 1.2\% \qquad (8.5)$$

c. Ductility Index μ_f

The curvature at the first yield of main reinforcement Φ_y and the curvature at ultimate loadΦ_u were measured (Fig. 20). The ductility index μ, defined by Φ_u/Φ_y, increases with the volume fraction of steel fibers as follows:

$$\mu_f \text{ (steel fibers)} = (1.12 + 11.8\ V_f - 4.75\rho V_f)\ \mu_{control} \qquad (8.6)$$

Eq. 8.6 is not valid for $V_f = 0$, but provides the best fit for the range of V_f used.

d. Plastic Rotation Capacity θ_p:

The plastic rotation of all beams were measured. The plastic rotation is defined by:

$$\theta_p = \int_0^{HL} (\Phi_u - \Phi_y)\, dx \qquad (8.7)$$

Where the term $(\Phi_u - \Phi_y)$ represents the plastic curvature. Thus knowing the curvature leads to determining the rotation. Figure 21 shows the distribution of the plastic curvature along the plastic hinge length at the intermediate support of one group of G3 beams, designed as singly reinforced (dashed lines) and a second group of G6 beams containing compression steel (solid lines). It can be observed that the presence of steel fibers enhanced the relative plastic rotation in both groups. Also, the addition of compression steel increased the relative plastic rotation appreciably. Analysis of the results led to the following prediction equation to evaluate the plastic rotation capacity:

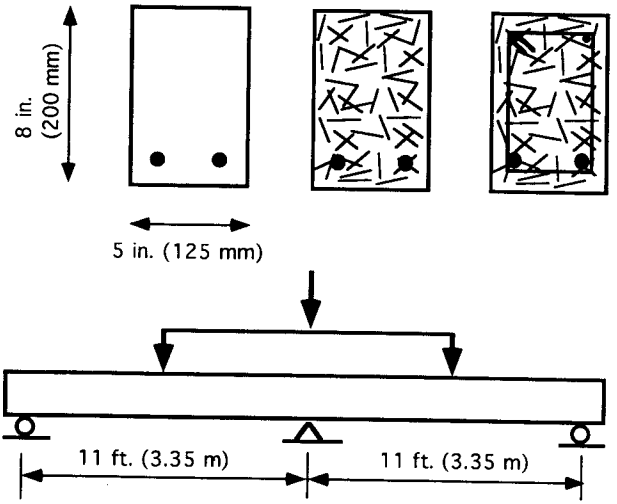

Fig. 19. Loading set-up and beam cross section.

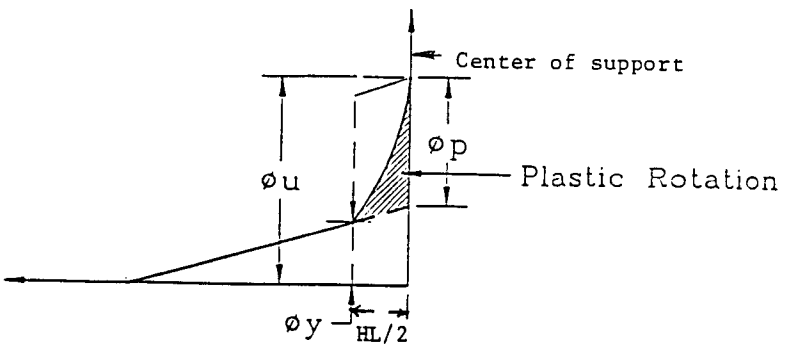

Fig. 20. Plastic rotation at first yield and at ultimate load.

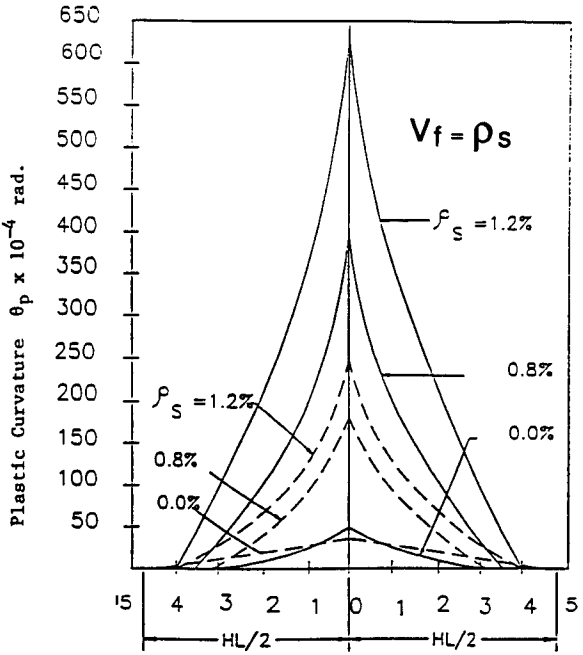

Fig. 21. Measured plastic curvatures versus distance from the center support from tests for: beams singly reinforced (dashed lines) and beams doubly reinforced (solid lines).

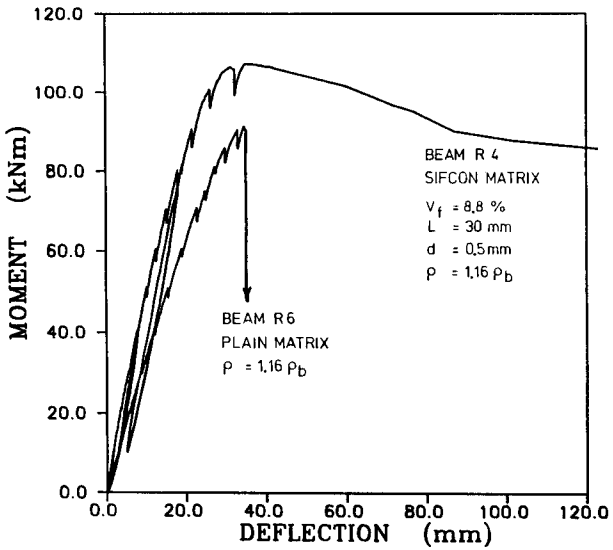

Fig. 22. Load-deflection curves illustrating the use of a SIFCON matrix instead of plain mortar.

$$\theta_p = (\Phi_u - \Phi_y)\,(HL)\,(\beta) = \frac{\text{Plastic Strain } \varepsilon_p}{k_u d}\,(HL)\,(\beta) \qquad (8.8)$$

$$\theta_p = \alpha\ \beta\ (0.003 / k_u) \qquad (8.9)$$

where

α = $(4.3 + 2.24\ V_f - 0.042\ f_y + 4.0\ \rho V_f)$ (8.10)

β = $(0.56 - 0.16\ V_f)$ (8.11)

k_u = $c / d = (\rho\ fy) / (0.85\ f_c'\ \beta_1)$ (8.12)

= ratio of the depth of the neutral axis to the effective depth d at ultimate load.

ε_p = plastic strain = $0.003 - \varepsilon_{py}$

ε_{py} = strain in concrete at first yield of steel

HL = from Eq. 8.4

e. Modulus of Rupture f_r

The modulus of rupture at the stage of initial cracking, f_{ri}, and at ultimate, f_{ru}, was determined from separate tests on beams according to ASTM C-1018. The following prediction equations were derived:

$$f_{ri} = (7.5 + 2.6V_f)\sqrt{f_c'} \qquad (8.13)$$

$$f_{ru} = (7.5 + 4.35V_f)\sqrt{f_c'} \qquad (8.14)$$

where

V_f = percentage of steel fibers by volume

f_c' = compressive strength of a standard concrete cylinder at 25 days.

7.3 Conclusions

Based on the results of the test program described in this Section, the following conclusions were drawn.

1. The presence of steel fibers in reinforced concrete beams increases the curvature substantially, relative to beams without fibers.
2. The length of the plastic hinge varied between *0.92d* and*1.04d* with an average of *d* for reinforced concrete beams without fibers, and between *1.15d* and *1.52d* with an average of 1.37d for beams with fibers.
3. A reduction in the tensile steel ratio ρ at the critical section increases the rotation capacity of plastic hinges, θ_p.
4. The extreme fiber compressive strain in concrete at ultimate load varied between 0.00307 and 0.0032 for beams without fibers, and between 0.0041 and 0.0058, for beams containing steel fibers with $V_f \leq 1.2\%$ by volume.
5. The presence of compression steel increased the relative rotation capacity appreciably as compared to singly reinforced concrete sections.
6. The plastic rotation capacity, plastic hinge length, curvature distribution factor and ductility index for fibrous reinforced concrete continuous beams can be estimated, as a first approximation, from the prediction equations suggested above.

8 Over-Reinforced RC Beams Using a Slurry Infiltrated Fiber Concrete (SIFCON) Matrix

The results of an experimental and analytical investigation of the behavior of nine reinforced concrete beams containing a SIFCON matrix were reported in [49]. Some

a)

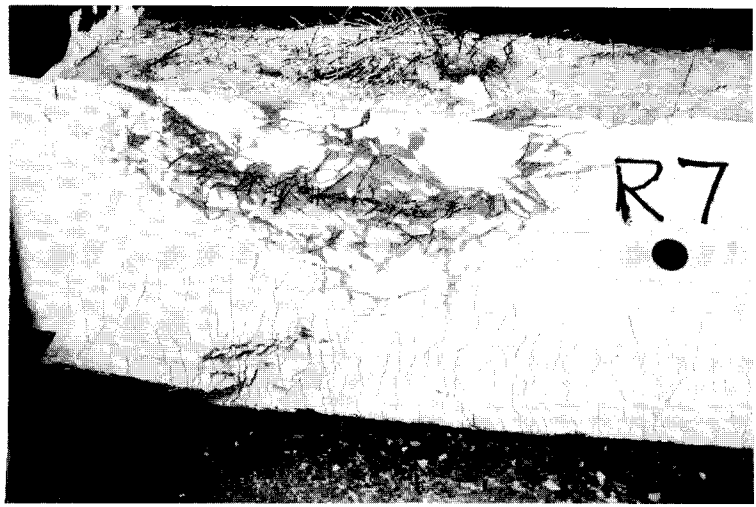

b)

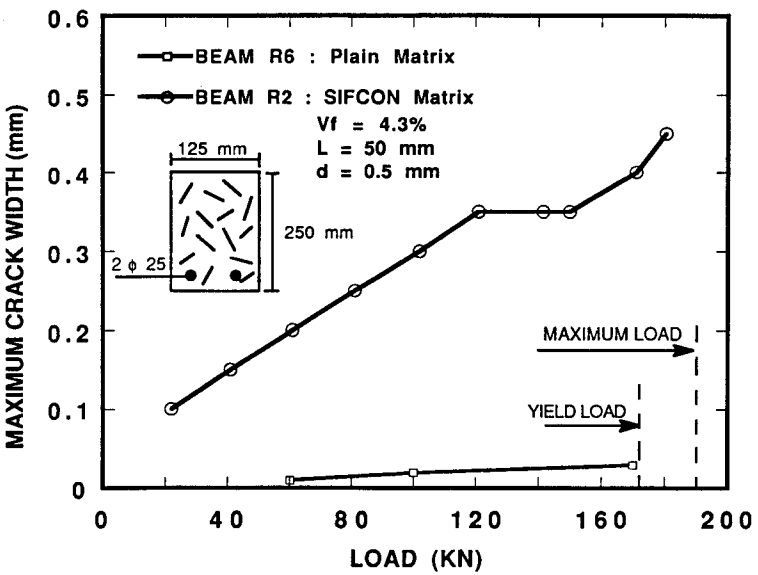

Fig. 23. a) Photograph of cracking at maximum load; b) comparison of maximum crack widths in reinforced concrete beams with a SIFCON matrix and a plain mortar matrix.

information on SIFCON preparation and applications is given in Section 11 of this Chapter. A summary of the main experimental observations is given next. A summary of the analytical modeling is described in Section 14 of this Chapter. The main objective of the study was to evaluate the effects of using a very ductile matrix, such as SIFCON, in over-reinforced concrete beams in order to improve their structural ductility. Another reason was to provide a means to achieve ductility with the use of high strength reinforced concrete. This is essentially achieved by using a ductile material in the compression zone of a beam in order to spread the zone of plasticity during failure. The beams had tensile reinforcement ratios (calculated assuming plain concrete matrix) ranging from 59% ρ_{max} to 350% ρ_{max}, where ρ_{max} is the maximum reinforcement ratio specified in the ACI Building Code. The effects of several variables were investigated, namely: the longitudinal bar reinforcement ratio, two different SIFCON matrices, the presence and absence of stirrups, rectangular and T-section behavior, the presence of compression reinforcement and the use of SIFCON only in the compression zone of the beam.

A typical moment-deflection curve illustrating the effect of using a SIFCON matrix instead of plain mortar matrix is shown in Fig. 22. It was generally observed that the presence of SIFCON in over-reinforced concrete beams leads to ductility indices exceeding three times those obtained using plain mortar, and energy absorption capacities exceeding four and one half times the energy obtained without SIFCON. The improvement in ductility was such that in some cases failure occurred by tensile failure of the steel reinforcement. Furthermore the maximum crack width and the average crack spacing were more than one order of magnitude smaller than in conventional reinforced concrete (Fig. 23). As an example, in one beam specimen, average structural crack spacing was about 13 mm, and maximum crack width was about 0.05 mm at yielding of the reinforcing bars.

The use of SIFCON changes the development of cracking in a conventional reinforced concrete member. Unlike for reinforced concrete, with SIFCON the number of cracks kept increasing with loading up to yielding of the steel reinforcing bars. This is similar to the property of multiple cracking particular to HPFRCC and has also been observed in ferrocement materials with high volume fraction and specific surface of mesh reinforcement.

Thus the use of SIFCON which was initially meant to improve the compression zone ductility of a reinforced concrete beam also led to improvements in its tensile zone behavior as well, by leading to very small crack widths, excellent crack distribution, and no spalling of the concrete cover (i.e. preserving bond) up to tensile failure of the bar reinforcement. Such a property can be used to improve the durability of the structure by protecting its tensile zone, and its seismic response by maintaining bond and related energy dissipation.

9 Effects of Fibers on Impact Response of RC Beams

9.1 Preparation and Test Setup

Within a research project granted by the European Community [20], beams were tested by Eibl and Lohrmann [21] to study the deformation behavior of medium-scale structural elements with and without steel fibers under both static and impact loading (Fig. 24). Nine reinforced concrete beams with the dimensions 200 x 250 x 2800 *mm* and a span of 2400 *mm* were cast. In all three matrix compositions were used: one plain concrete mixture containing a maximum aggregate size of 16 *mm* and two types of steel fiber concrete mixtures with a fiber content of 1.2% by volume:

- plain concrete mixture grade C30/37 (acc. to Eurocode 2)
- Dramix steel fibre: smooth wire 60 *mm*/0.8 *mm*, with hooked ends
- Wirex steel fibre: smooth straight wire 40 *mm*/0.6 *mm* (length, diameter)

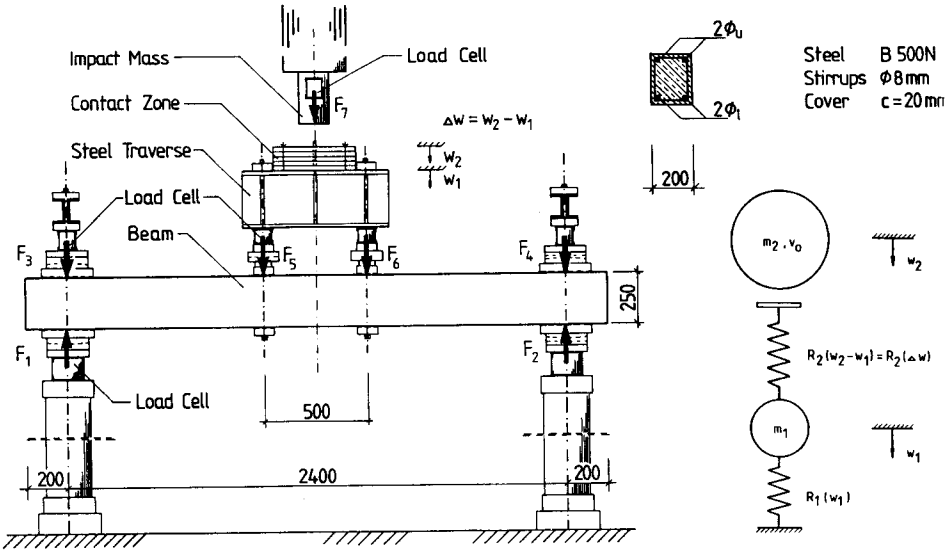

Fig. 24. a) Beam test set-up for impact testing and typical reinforcement arrangement for static and impact loading; b) TDOF substitute system

Table 3. Material properties under static loading for calculation of test series T1 and T2

Type of Mixture	Test Series T1 Plain	Dramix Fibre	Wirex Fibre	Test Series T2 Plain	Dramix Fibre	Wirex Fibre
Concrete Mixtures:						
Cylinder Strength, f'_c [MPa]	36.7	38.3	37.2	43.1	36.1	44.3
Young's modulus, E_c [MPa]	34000	34000	34000	34000	34 000	34000
Tensile Strengths: f_{f1} [MPa]	-	1.5	1.1		1.5	1.1
f_{f2} [MPa]	-	1.5	1.3		1.5	1.3
Reinforcement:						
Yielding Stress, f'_y [MPa]	564			561		
Young's modulus, E_S [MPa]	202000			202000		
Cross Ssections: A_{sl} [cm2]	3.01			0.982		
A_{su} [cm2]	1.006			0.566		

Table 4. Toughness indices for statically loaded beams (ASTM C 1018).

Mixture	Series T1*		Series T2**	
	I_5	I_{10}	I_5	I_{10}
Plain	4.43	8.59	4.7	9.3
Dramix fibre	4.56	9.64	4.6	9.1
Wirex fibre	4.54	9.04	4.6	9.0

* test results; ** prediction

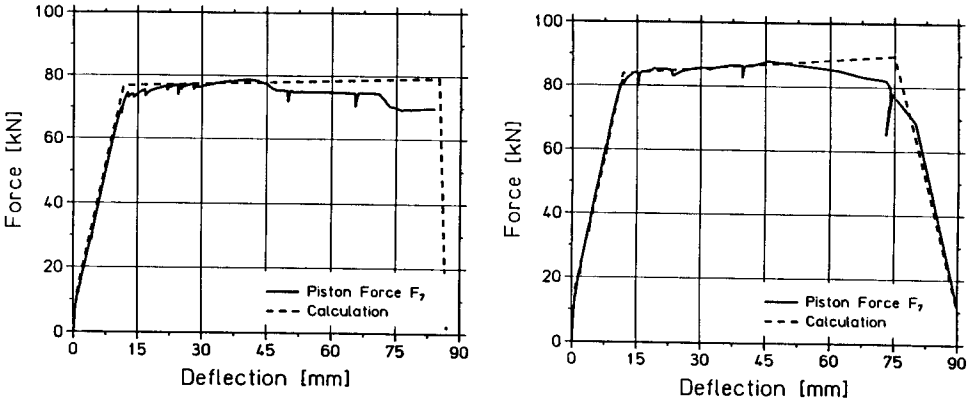

Fig. 25. Static load-deflection curves for test series T1 for: a) control beam with plain concrete; b) beam with FRC (Dramix) mixture

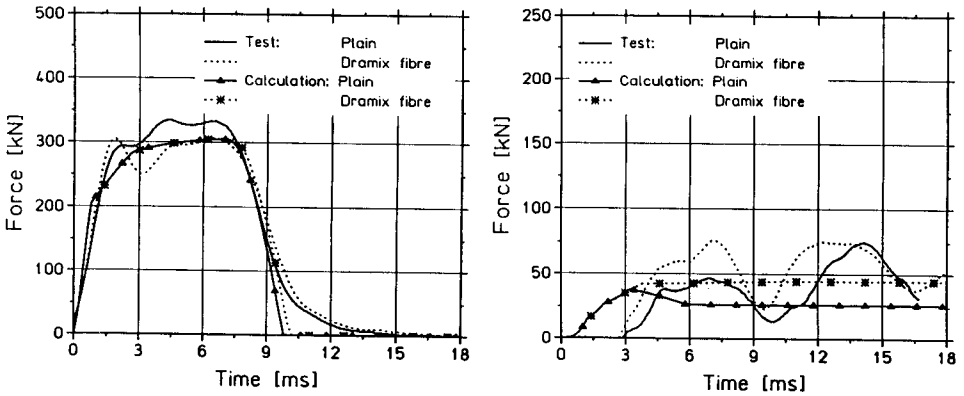

Fig. 26. Force versus time curves under impact loadding for test series T2: a) contact zone; b) gravity supports.

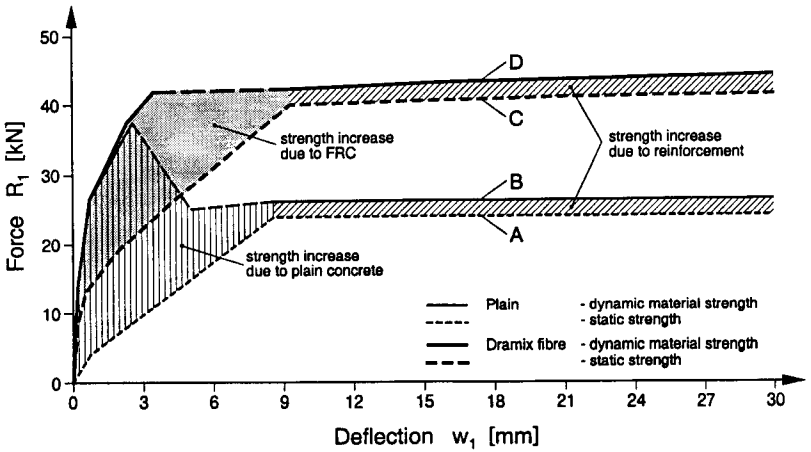

Fig. 27. Details of load-deflection curves of test series T2 for both control and fiber reinforced concrete (Dramix) beams using static material strength (A,C), and dynamic material strength (B,D).

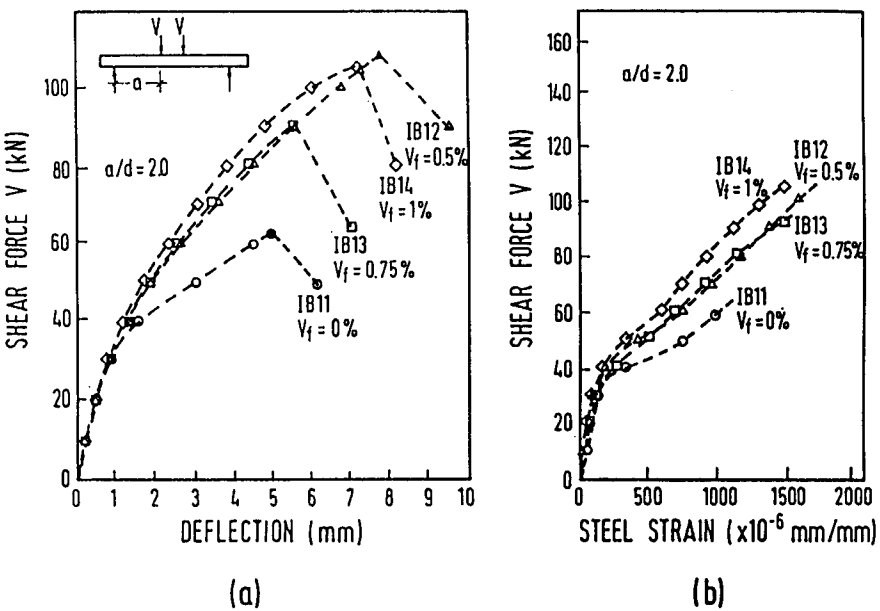

Fig. 28. Response of reinforced steel fiber concrete beams with varying steel fiber content.

The reinforcement in the tension zone consisted of 2 bars of either 14 *mm* (test series T1) or 8 *mm* (series T2) in diameter. A strong stirrup reinforcement ensured that the beams could not fail by either punching or shear. The load was applied by a stiff steel beam over two points located 500 *mm* apart.

For the static loading case, the load was applied by a displacement controlled hydraulic testing machine. Material properties were determined from cores drilled from reference specimens, and from samples of the reinforcing steel (Table 3). In all cases, the testing age was 28 days.

The setup for impact tests is shown in Fig. 24. The beams were loaded by a drop weight of 1080 *kg* falling from a nominal height of H_{nom} = 2.0 to 2.2 *m* . The load-time function of the hard impact was smoothed due to a special arrangement of the contact zone. After about 16 to 23 *ms* , auxiliary supports at midspan stopped the beam's movement. Data was registered with transient recorders in 1 micro-second intervals.

9.2 Experimental Results

Results of one typical fibre mixture (Dramix) are plotted together with the corresponding values for plain concrete at different types of loading.

9.2.1 Static Loading

The load (F_7) versus midspan deflection curve for the static test of series T1 is plotted in Figs. 25a and 25b for the plain and the Dramix fibre mixture, respectively. Predicted curves from an analytical model developed by Eibl and Lohrmann are added, based on the material properties listed in Table 3. The stress-strain relationship of the concrete was assumed to be parabolic with an initial Young's modulus E_c = 34 000 MPa.

Figure 27 shows that the load capacity for the second series (T2) increases between 50 and 65% due to addition of fibers (curve B) compared with the plain concrete mixture (curve A). Toughness indices measured according to ACI [6] and ASTM C 1018 are summarized in Table 3.

9.2.2 Impact Loading

A two-mass (TDOF) system was used for the numerical simulation of the beam's behavior under hard impact. Strength increase of concrete [9] and mild steel [15] due to high strain rates were included in the characteristic of the lower spring R_1, representing the nonlinear load-deflection behavior of the beam (Fig. 24b).

In Fig. 26a load-time curves of test (F_7) and calculation (R_2) are compared for plain and Dramix fibre mixtures for test series T2. The development of spring force (R_1) and measured support forces ($F_1 + F_2$) at the end of the beam can be obtained from Fig. 26b. Comparing both curves, it is noted that the curve calculated for R_1 represents the contribution of the main bending mode. Higher modes are visible in the measured values of the support forces. A comparison of the time evolution of the calculated forces with the measured ones showed, however, that the total momentum transferred to the supports is the same.

Fig. 27 shows a detail of the calculated load-deflection curve of both plain and the Dramix fibre mixture of series T2. The behavior under static loading based on the static material properties is given by curves A (plain mixture) and C (fiber mixture). Curves B and D were calculated using the dynamic material properties.

It should be noted that the dynamic strength increase of concrete is mainly limited to its uncracked phase [20] (see also Fig. 24 in Chapter 6), which is equivalent here to a midspan deflection of about 3 *mm*; this deflection is reached within nearly 4 *ms* after onset of loading. Up to this value, for fibre mixtures of series T2, more than 85% of

the beam's resistance results from the fibre reinforced concrete, and 15% from the mild reinforcement.

10 Effects of Fibers on Shear Response of RC and PC Beams

10.1 Introduction

The addition of discrete steel fibers helps to improve the post cracking behavior of concrete materials, and leads to improvement in the shear behavior of reinforced concrete (RC) and prestressed concrete (PC) beams. A research program was carried out at the National University of Singapore by Paramasivam et al. [75] to study the effectiveness of steel fibers as shear reinforcement in reinforced and partially prestressed concrete beams. A brief summary is given here; details can be found in Refs.[34,35,36,39,40,41,55,66,67]. The shear behavior can be predicted using the following concepts:

1. Methods based on plasticity analysis [34]
2. Methods based on the constitutive relations of the material components [66]
3. Semi-empirical methods leading to equations predicting the ultimate strength of beams [34] by characterizing the influence of steel fibers

These concepts are discussed in the following sections.

10.2 Method Based on Plasticity Analysis

Lim et al [35,26] proposed a method based on plastic analysis to predict the ultimate strength of fiber reinforced RC beams under combined bending and shear. The beam after diagonal cracking, was modeled as a truss with the steel fiber concrete between diagonal cracks acting as compression struts and the web reinforcement (stirrups) as the vertical tension members. The influence of steel fibers was modeled using the post cracking tensile strength of fiber concrete. The observed failure loads and modes of failure for 22 test beams agreed well with the predictions. The results suggest that fibers can replace vertical stirrups either partially or completely as long as parity in the shear reinforcement factor is maintained.

10.3 Analytical Models Based on Constitutive Relations

The inclusion of steel fibers in concrete increases the resistance to crack growth which, in turn, results in reduction of principal tensile strains and consequently increases the ultimate capacity. Constitutive models for steel fiber concrete under biaxial compression-tension [39] and under biaxial compression [68] have been developed for modeling in the finite element method [40,41]. Using the constitutive relations for steel fiber concrete under biaxial compression-tension, an analytical model based on the modified compression field theory (MCFT) was proposed to predict the response of beams under shear and bending [66,68]. Although this method is computationally easy, the assumption on the shear stress distribution and the variation of longitudinal strains limits its general applicability. A non-linear finite element analysis (FEM) incorporating the constitutive relations for steel fiber concrete has also been developed. The finite element formulation uses the concept of smeared rotating crack model and the solution is obtained by the secant modulus approach. The predictions of both approaches have been verified by an experimental program on RC and PC beams. Parameters such as volume fraction of fibers, partial prestressing ratio and shear span to depth ratio were considered in the experimental program.

10.4 Semi-Empirical Equation of Ultimate Strength

Several equations have been proposed in the past by different authors for predicting the ultimate strength of steel fiber concrete beams under bending and shear. The ultimate

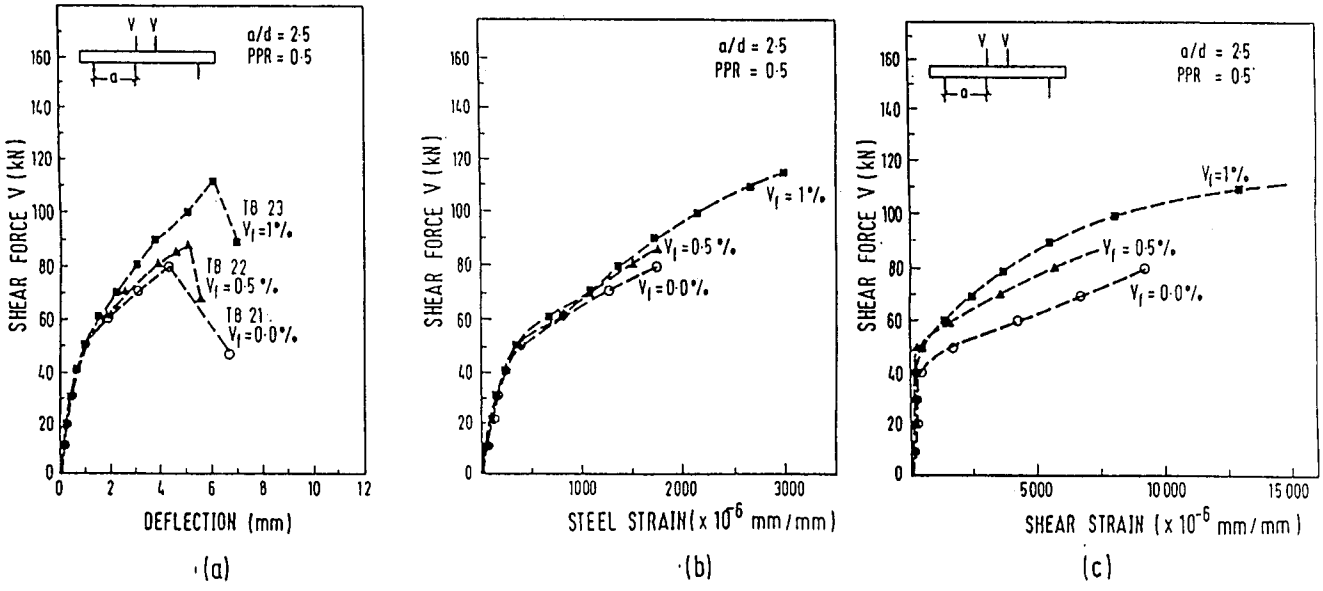

Fig. 29. Response of partially prestressed beams with varying steel fiber content.

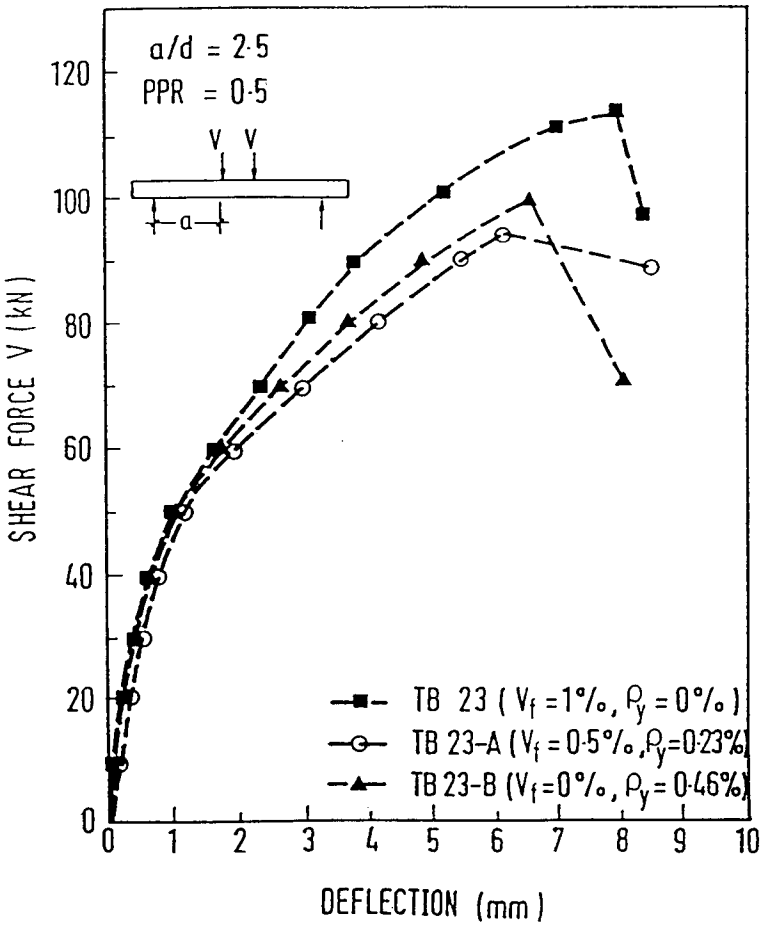

Fig. 30. Load-deflection curves of beams with different combinations of fibers and stirrups used as shear reinforcement.

strength equations of reinforced and prestressed concrete elements were modified to incorporate the influence of steel fibers. The ultimate shear carrying capacity (V_U) of the concrete beams can be taken as the sum of the shear force carried by concrete (V_C), the shear force carried by stirrups (V_{ST}) and shear force carried by steel fibers (V_{SF}), that is:

$$V_U = V_C + V_{ST} + V_{SF} \tag{8.15}$$

Assuming the traditional 45° truss model, the contribution of vertical stirrups can be determined as in the ACI Building Code 318-1992 [5]:

$$V_{ST} = \rho_y (f_{yv}) b_w d \tag{8.16}$$

where ρ_y is the stirrup reinforcement ratio = $A_v/b_w S$; A_v is the cross-sectional area of vertical stirrup; S the spacing, f_{yv} the yield strength of the stirrups; and, b_w and d the width and depth of the beam respectively. The contribution of concrete V_C can be obtained using the ACI Code [4]. The contribution of steel fiber can be estimated from the following equation [39,66]:

$$V_{SF} = 0.6\, \sigma_{pc}\, b_w d \tag{8.17}$$

where σ_{pc} is the post-cracking tensile strength of steel fiber concrete under uniaxial tension (see Chapter 1 in this Volume).

10.5 Results and Conclusions

Six reinforced concrete beams and ten prestressed concrete beams with different parameters such as volume fraction of fibers (V_f), shear-span to effective depth ratio (a/d), partial prestressing ratio (PPR) and stirrup reinforcement ratio (ρ_y) have been tested. The experimental results were compared with analytical predictions by the modified compression field theory (MFCT), the finite element analysis (FEM) and the semi-empirical equations. Figures 28 to 30 show the influence of fiber content on the behavior of the RC and PC beams respectively [39,55,68]. The following conclusions were drawn:

1. The shear capacity increases with an increase in steel fiber content. The increase can be as much as 70% with the addition of 1% steel fibers by volume of concrete.
2. Steel fibers substantially improve stiffness after web cracking. This is because the steel fibers act as crack arrestors and contribute to the tension stiffening of concrete.
3. The web cracking load was mainly influenced by the shear-span to effective depth ratio and the partial prestressing ratio of the beams.
4. For design purposes, a simple semi-empirical equation, leading to a conservative estimate of ultimate strength, can be used along with the ACI code equation.

11 Cyclic Shear Response of Dowel Reinforced Slurry Infiltrated Fiber Concrete - SIFCON

11.1 Introduction and Objectives

Slurry Infiltrated Fiber Concrete (SIFCON) differs from conventional fiber reinforced concrete in terms of fabrication and composition. In SIFCON the fibers (primarily stiff fibers such as steel fibers) are pre-placed in the mold to its full capacity thus forming a network, then the fiber network is infiltrated by a cement based slurry [42]. Because of this method of fabrication, the volume fraction of fibers can be very high, ranging from 4% to 25%, and is a function of several parameters that include the shape, diameter, and aspect ratio of the fibers, their orientation, the method used in packing, mold size and extent of vibration. The slurry based matrix must be made of sufficiently fine particles to infiltrate the fiber network.

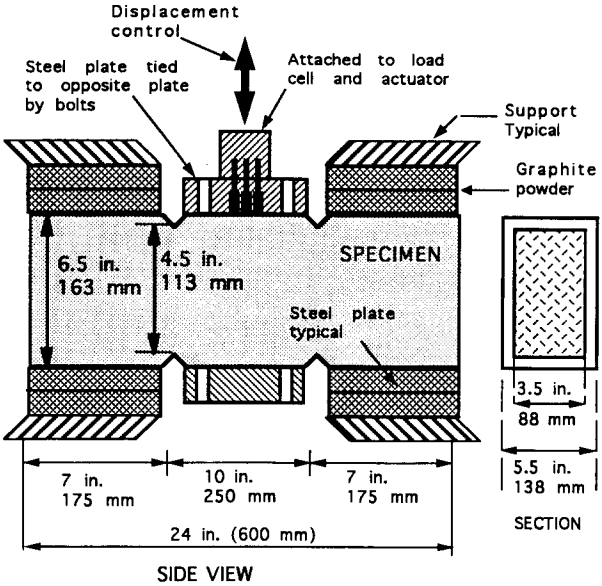

Fig. 31. Typical double shear specimen used to evaluate cyclic response in shear.

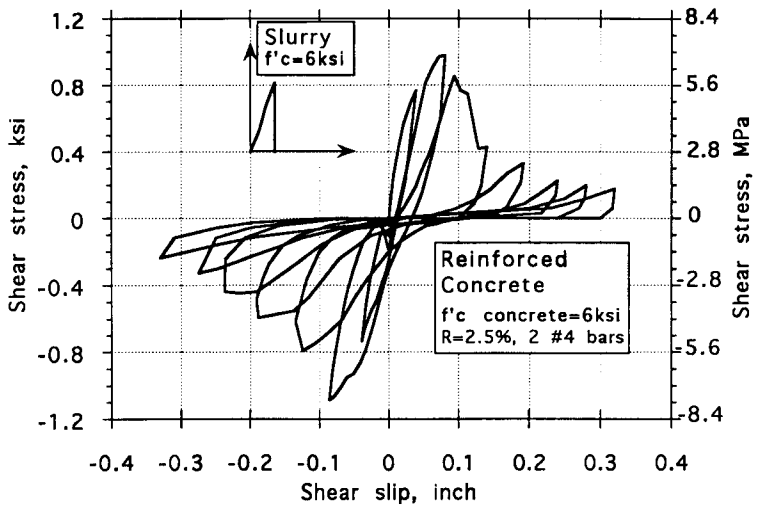

Fig. 32. Response of dowel reinforced concrete specimen without fibers under cyclic shear.

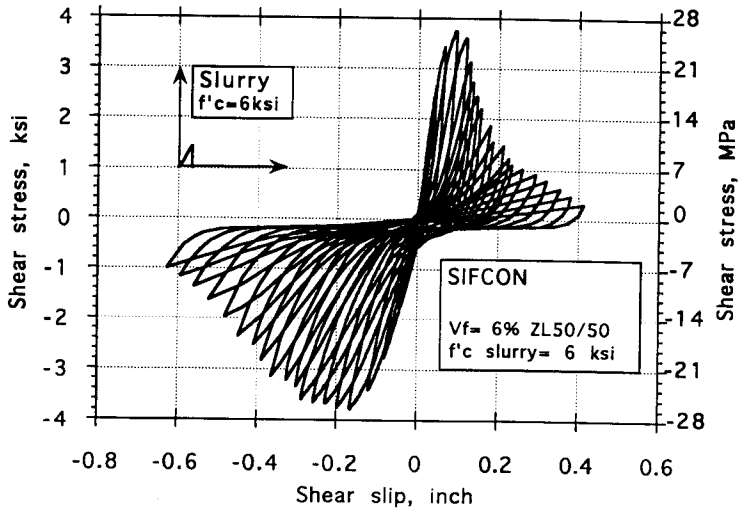

Fig. 33. Typical response of SIFCON without reinforcing bars under cyclic shear loading and comparison with plain matrix.

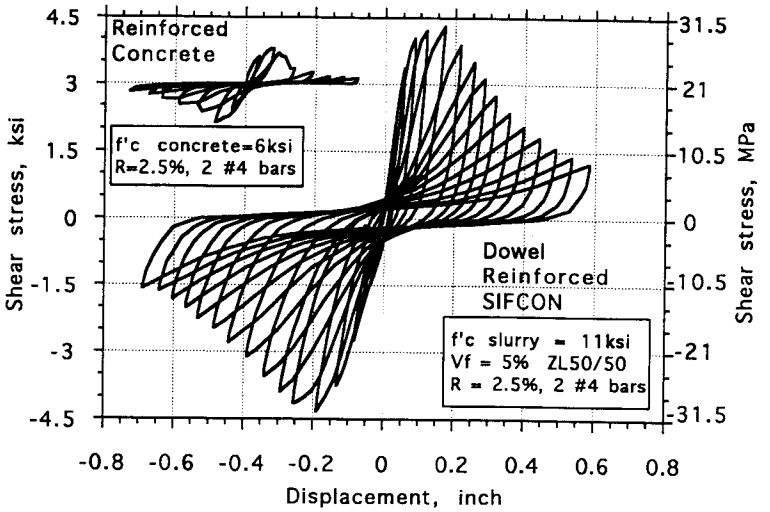

Fig. 34. Comparison of cyclic response in shear of dowel reinforced SIFCON and dowel reinforced concrete.

SIFCON has several potential benefits in structural applications where it can be used either in the full structure (i.e. shear wall) on in part of it, such as in a member or a joint. It can also be used in repair applications such as in patching, pot-holes, and bridge decks. Several investigations have addressed the mechanical properties of SIFCON as a material in tension, compression, bending and shear [42,45,46]; there is increased interest in using SIFCON in combination with reinforcing bars and prestressing tendons, when its improved properties justify its additional cost (see Sections 8 and 13 in this Chapter). The use of SIFCON may be particularly advantageous in seismic resistant structures subjected to extreme cyclic loading.

A study by Naaman and Baccouche [43,44] have focused on the shear response of SIFCON and dowel reinforced SIFCON subjected to monotonic and cyclic loading. The overall objectives of the research were: 1) to investigate the shear response and energy absorbing capacity of SIFCON in shear with and without dowel bar reinforcement, under monotonic and cyclic loading; 2) to examine the contribution of fiber volume fraction, dowel reinforcement ratio, and slurry compressive strength, to the shear strength and fracture energy of SIFCON; and 3) to develop an analytical model to predict the shear stress-displacement response of SIFCON subjected to monotonic and reversed cyclic loading. The test set-up is shown in Fig. 31. Only some of the experimental observations and related conclusions are presented in this summary. Details can be found in [43,44].

11.2 Results and Conclusions

Typical results are illustrated in Figs. 32 to 34. Figure 32 shows the cyclic shear stress versus displacement response of the dowel reinforced concrete specimen without fibers; Fig. 33 shows the cyclic response of SIFCON without reinforcing bars, and in insert, plotted on the same scale, the monotonic response of the slurry matrix. Fig. 34 shows the cyclic response of dowel reinforced SIFCON as compared (in insert plotted on the same scale) with dowel reinforced concrete using same dowel reinforcement ratio. The shear stress was defined as the shear force divided by the gross area. Related salient conclusions were as follows.

1. The shear strength (maximum observed shear stress) of dowel reinforced SIFCON ranged from 2.7 to 3.5 times that of dowel reinforced concrete with same dowel reinforcement and same compressive strength. The equivalent shear strength of dowel reinforced SIFCON exceeded 30 MPa.
2. The energy absorbed by dowel reinforced SIFCON specimens tested under reversed cyclic loading was found to be 10 to 15 times that of dowel reinforced concrete.
3. The shear strength of SIFCON and dowel reinforced SIFCON specimens subjected to reversed cyclic loading ranged from 80% to 95% of that of the monotonically tested specimens.

12 Behavior of Prestressed SFRC under Tension Release

12.1 Introduction

Rapidly developing building industry requires new and economical construction technologies and high-tech materials all over the world. In particular, steel fiber reinforced concrete (SFRC) is believed to improve the behavior of conventional concrete structures. However, so far only few investigations have dealt with the behavior of SFRC in structural reinforced concrete members [7,8,26,28,36,53,66], partially prestressed members [26] and axially prestressed members [72]. Tests were also carried out to investigate the punching strength of prestressed SFRC flat slabs [69] as well.

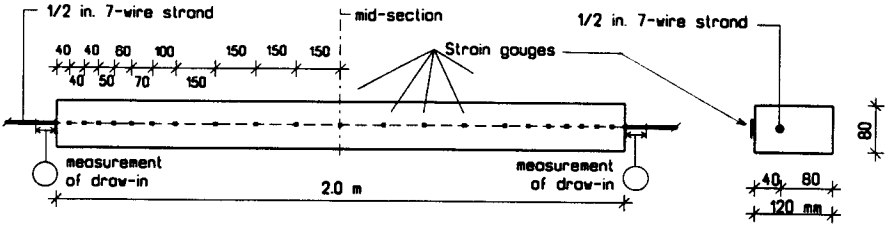

a, Test specimen

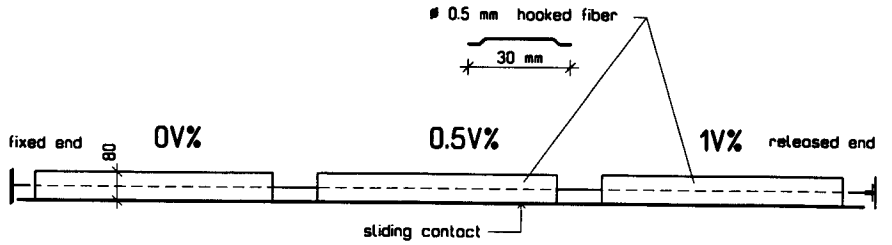

b, Test arrangement

Fig. 35. Test sepcimens and testing bed arrangement.

Table 5. Test variables for Test Group "B"

Series	Number of specimens	Specimen No.	Steel fiber content [V%]	End block reinforce-ment	f_c [N/mm^2]	Type of tension release
1	3	No.1 No.2 No.3	0 0.5 1.0	no no no	37.5 39.8 38.6	gradual
2*	3	No.1 No.2 No.3	0 0.5 1.0	no no no	- - -	sudden

*ongoing tests

12.2 Research Significance

In the case of prestressed pretensioned structural members the reliable determination of the transfer length of prestressing tendons is an important issue both for the end block design and for the analysis of the structural member under load. The transfer length of a prestressed pretensioned concrete member is defined as the length required to develop the effective prestress in the tendon by bond. The transfer length is affected by many factors, such as strength of concrete, degree of compaction, transverse reinforcement in the end block, size and type of tendon, type of tendon release, etc.

Short transfer lengths are unfavorable for the end block design, while long transfer lengths decrease the moment and shear capacity of the members. End block design needs special care because severe splitting cracks may develop during the release of the prestressing force, especially for a relatively low concrete tensile strength or in the absence of proper end reinforcement. Moreover, the release of prestressing force (at cutting of the tendons) often induces an impact load to the end block.

It is believed that the use of SFRC in prestressed pretensioned structural members may: 1) improve concrete quality, 2) help to resist sudden impact load at prestressing force release, 3) and reduce or substitute for end block reinforcement while preventing end block cracking.

12.3 Experimental program

Sixteen prestressed pretensioned concrete beams were tested in the Department of Reinforced Concrete Structures, Technical University of Budapest, Hungary by Balazs and Erdelyi [73]. Since each beam has two ends, 32 data groups were studied, 8 of which containing steel fibers.

12.3.1 Test variables

Beam specimens having 80*120 mm cross-sectional area and prestressed by a 12.7 mm diameter, straight seven-wire steel strand were prepared. The beams were two meters long. The strand was placed eccentrically as shown in Fig. 35. The strand had the following properties: a nominal tensile strength of 1770 N/mm^2; a nominal yield strength of 1550 N/mm^2; and a cross-sectional area of 100 mm^2. When fibers were used, there was no longitudinal reinforcement, other than the strand, and no stirrups.

Concrete mixes for all specimens were made by the same mixing method. Steel fibers were added after mixing conventionally. Extra mixing with fibers took another 5 minutes. Hooked steel fibers (trade name DRAMIX), 30 mm long, 0.5 mm in diameter, and with an aspect ratio of 60 were used in volume fractions of 0.5% and 1%. This was equivalent to a fiber content of respectively 39.2 kg/m^3 and 78.4 kg/m^3.

All specimens were compacted at the place of prestressing with the same time and compaction method and with a 40 mm needle vibrator. The specimens were kept wet for 14 days after casting and tested at 28 days after casting.

The tests were carried out into two groups, identified as Group A and Group B. Details for Group A are given in [69] while those of Group B are described in [73]. Six beams from Group B contained steel fibers; three were tested with sudden release of prestress and three with gradual release of prestress (Table 4). Below only results related to the beams with gradual release of prestress are described.

12.3.2 Concrete compressive strength

Concrete compressive strengths measured on 150 mm cubes (average of 6 cubes for each steel fiber content) for V_f = 0, 0.5 and 1.0 % were 37.5, 39.8 and 38.6 N/mm^2, respectively. The corresponding Young's moduli were 45400, 41500 and 38700 N/mm^2, respectively, showing a decrease in Young's modulus with increasing fiber content.

12.3.3 Measuring system

Concrete strains were measured with 20 mm long strain gauges placed along the most compressed surface of the members. Strain gauge arrangement followed the change of the prestressing force. Shorter strain gauge spacings were applied at the end blocks and longer spacings in the middle portions of the specimens.

For the determination of the strand draw-in, steel rings were fixed to the strand as well as to the butt end of the elements having three imprinted steel balls on each rings in the same position. Steel ball distances were measured during the tension release with a mechanical measuring device having 0.005 mm sensitivity. After subtracting the strand elongation from the measurements, strand draw-in was determined (Fig.36a).

The camber of each member as influenced by the prestressing force at release, was also measured by dial gauges, of 0.01 mm sensitivity, placed at the middle section and at the two ends.

12.4 Test Results with Gradual Tension Release

12.4.1 Prestressing force versus draw-in

Prestressing force was released in 9 steps from 135.8 kN to zero. Note that since the cross-sectional area of the strand was 100 mm^2, 100 kN of prestressing force corresponds to a stress in the strand of 1000 N/mm^2 (1000 MPa).

The released prestressing force versus draw-in relationship for 1.0 % fiber content is presented in Fig. 36a. The two dotted lines indicate the measurements on the active and on the passive sides of the specimen (i.e., on the side of tension release and on the side of the fixed end, respectively). Mean value of the active and passive side measurements was corrected to account for the elongation of the strand between the two measuring points (Fig. 35). Non-linear relationship for the released prestressing force versus draw-in (continuous line) was obtained from the measured values. These relationship are compared for 0, 0.5 and 1.0 % fiber contents in Fig. 36b. Each curve gives the average of two measurements.

It can be observed that the addition of fibers generally produces a lower draw-in of prestressing strand. Draw-in results for 0.5% and 1.0% fiber contents are not considerably different from each other. For 1% fiber content, the decrease in strand draw-in at different released prestressing force levels was as follows:

Released prestressing force [kN]	Reduction in draw-in compared to plain concrete [%]
35	48
55	32
75	27
95	22
105	16
115	18
125	14
136	16

Therefore, the decrease of strand draw-in within the practical range of 950 to 1250 MPa prestressing steel stress, was only between 14 and 22 %. This is relatively small, but indicates a possible trend when higher fiber contents are used.

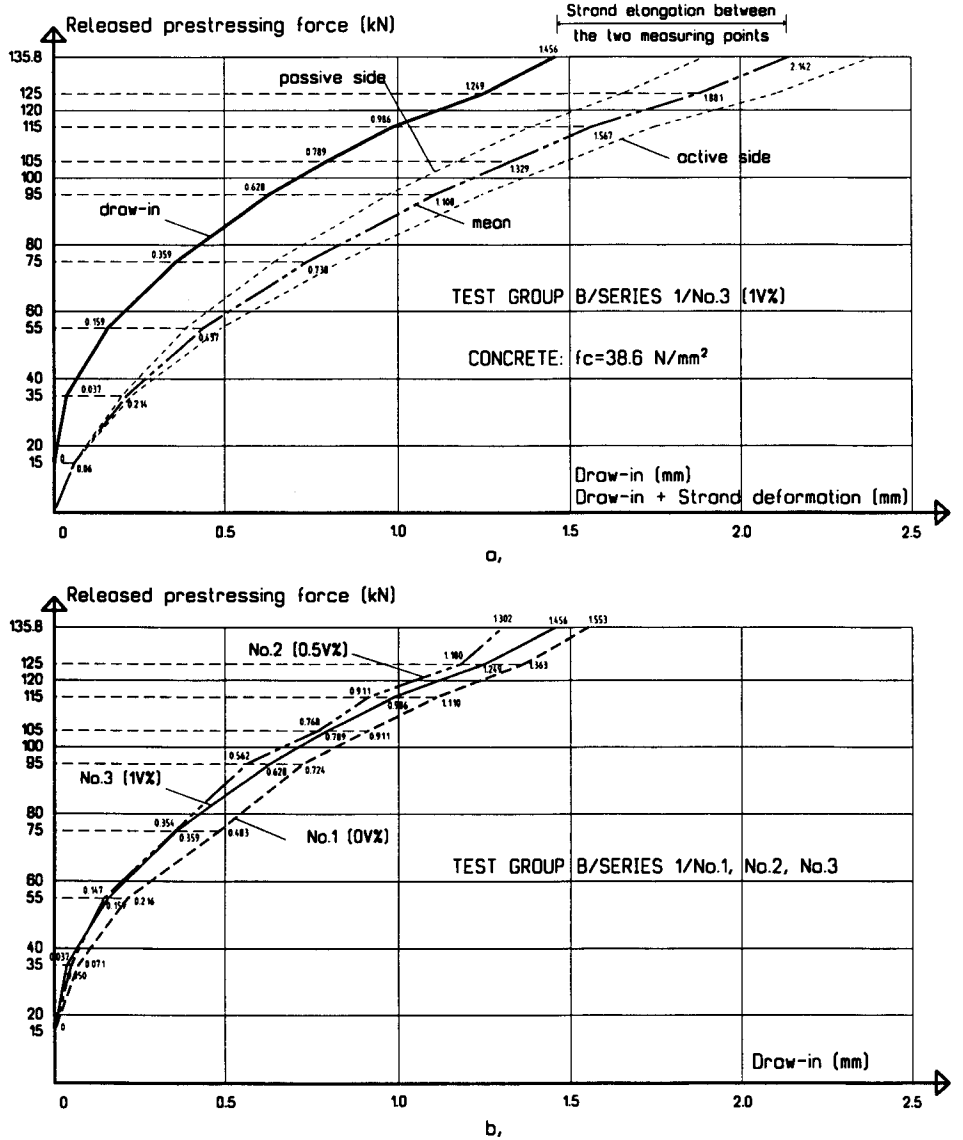

Fig. 36. Released prestressing force versus draw-in: a) measured and corrected curves for $V_f = 1\%$; b) average curves for $V_f = 0$, 0.5% and 1%.

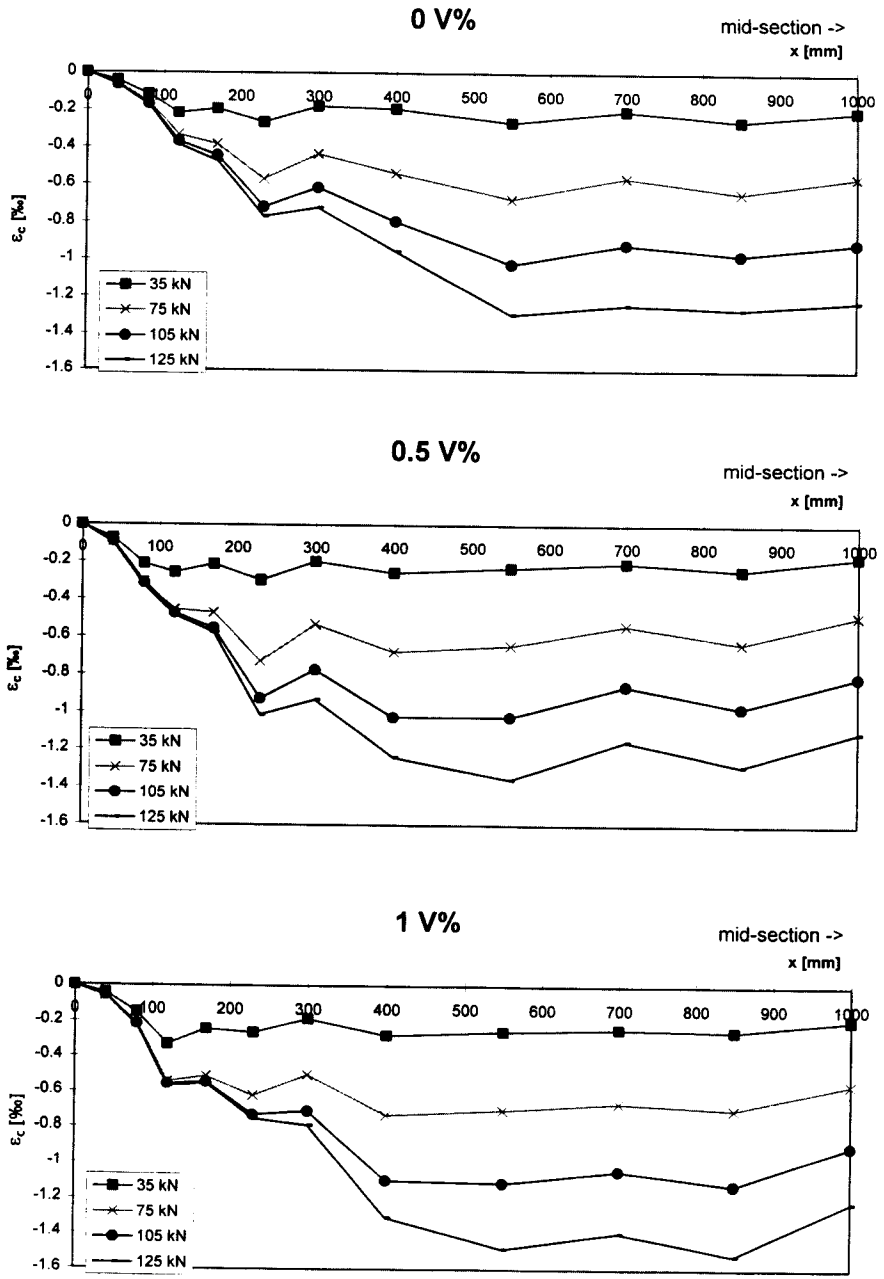

Fig. 37. Concrete strain measurements along the specimen during release of the prestressing force for $V_f = 0$, 0.5% and 1%.

12.4.2 Strain measurements

The eccentricity of the prestressing force was equal to the lower limit of the central kern of the section. Therefore, the entire section was compressed having the neutral axis (zero stress point) just at the extreme fiber of the section farthest from the strand.

The concrete deformations were measured with strain gauges on the most compressed concrete surface. The arrangement of strain gauges is given in Fig. 35 Strain measurements on specimens with 0, 0.5 and 1.0% steel fiber contents are presented in Fig. 37 according to four different levels of the released prestressing force. Each curve gives the average of the measurements on the active and passive sides plotted over half the specimen. The comparison of strain measurements indicates that the development of prestressing force needs shorter lengths when steel fibers are used.

Shorter development of the prestressing force with lower draw-in values can be explained by the effect of steel fibers reducing micro-cracking in the bond region.

12.4.3 Camber

Camber of the mid-section was monitored during tension release and over the next 165 hours. Comparison of measurements indicates that increasing steel fiber contents may lead to an increase in camber both during tension release and later. Lower Young's moduli and shorter transfer length may explain the increase of camber with increasing fiber content. Indeed, the ratio of measured camber of the specimen with 0.5 and 1.0 % steel fibers to that of the control specimen with no fibers, was about of the same order as the inverse ratio of their Young's moduli.

12.5 Conclusions

The following conclusions were drawn.

1) The addition of steel fibers produces lower draw-in of the prestressing strands. The observed decrease within the practical range of 950 to 1250 MPa prestressing stress ranged from 14 to 22 % compared to the draw-in of the control specimens without fibers. Observed draw-in values for specimens with 0.5 and 1.0 V% steel fiber contents were not considerably different.
2) Test results showed a decrease in the transfer length of the prestressing strand with addition of fibers.
3) The addition of fibers does not necessarily reduce camber of the prestressed concrete members. Both the Young's modulus of the matrix and the actual value of the transfer length have an important influence on the camber at mid-section.
4) Application of fiber reinforcement in pretensioned concrete members may be especially effective at the end blocks, where high tensile splitting stresses arise with the application of the prestressing force.

It should be observed, that since the volume fraction of fibers used in this study was small ($\leq 1\%$), the behavior of the beams tested is only indicative of the potential trends that may be obtained by adding fibers in the end blocks of prestressed concrete beams. Higher fiber contents, leading to high performance fiber reinforced concrete matrix with strain hardening and multiple cracking behavior, should lead to significantly improved properties of the end block.

13 Ductility of Beams Prestressed with Fiber Reinforced Plastic Tendons

The potential use in reinforced and prestressed concrete structures, of fiber reinforced polymeric (or plastic) reinforcements (FRP) utilizing high performance fibers such as carbon, glass, aramid (kevlar), and others, is gaining increased attention. FRP reinforcements were developed to replace conventional reinforcing bars and prestressing

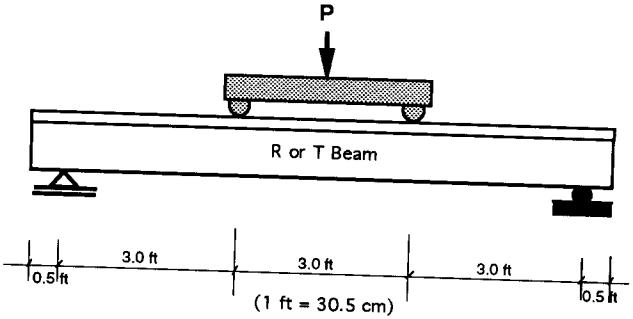

ω = global reinforcing index
PPR = partial prestressing ratio
CFCC = carbon fiber composite cable (prestressed)
The steel strands or bars are not stressed.
SIFCON = slurry infiltrated fiber concrete.

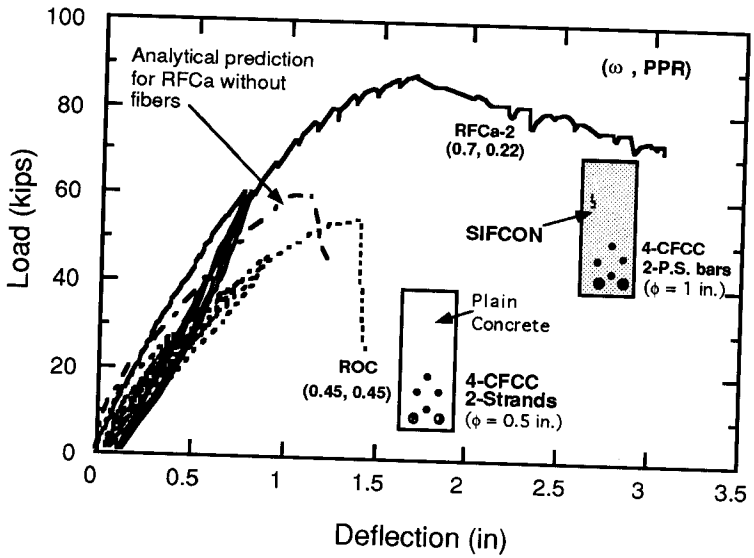

Fig. 38. Load deflection curves of over-reinforced prestressed beams with plain concrete matrix and with a SIFCON matrix (the beams are prestressed with carbon fiber tendons).

tendons. They are seen primarily as a means to avoid corrosion problems otherwise encountered in concrete structures reinforced with conventional steel reinforcing bars or steel prestressing tendons, and in applications involving magnetic impermeability. However, FRP reinforcements show linear elastic brittle behavior up to failure; their use in conventional concrete structures raises a serious concern about the lack of structural ductility which must be fully addressed in design [46].

Several methods have been devised by Naaman and Jeong to improve structural ductility in beams prestressed with FRP tendons [47,48]. One approach is to use over-reinforced beams, forcing failure in the concrete compression zone, which is reinforced with discontinuous fibers. The use of fibers increases the strain capacity of the matrix in compression and spreads the extent of the plastic hinge at failure, leading to improved ductility.

The behavior of four control test beams prestressed with CFCC (Carbon Fiber Composite Cables - Trade name CFCC by Tokyo Rope) tendons were evaluated particularly for ductility and compared with that of a beam prestressed with steel strands. Results show that the beams with CFCC tendons have a lower ductility index than the beam with steel strands. However, their ductility can be substantially improved by using a fiber reinforced concrete matrix to increase the strain capacity of the concrete.

Figure 38 shows the load-deflection curves observed for two typical beams. Beam ROC, cast with ordinary concrete, and prestressed with carbon fiber composite tendons underwent a brittle flexural compression failure. However, RFCa-2, also prestressed with CFCC tendons, but made from SIFCON, showed a ductile behavior without any sudden drop in the load-carrying capacity. The ductility index calculated based on energy considerations [47] was about 1.4 for beam ROC and 3.9 for beam RFCa-2 implying that the use of fiber reinforcement led to a more than one hundred percent increase in structural ductility. Moreover, neither of the CFCC tendons failed at maximum load.

It is concluded that the use of discontinuous fibers in concrete structures reinforced or prestressed with fiber reinforced plastics (FRP) reinforcement is an effective method to improve the overall structural ductility of these structures and will open up their applicability in real practice.

14 Structural Modeling

14.1 Nonlinear Analysis and Constitutive Relations

The behavior of reinforced and prestressed concrete structural elements can be accurately predicted using currently available methods of non-linear analysis [50,51]. Such methods are based on a number of acceptable assumptions such as plane sections remain plane after bending, and perfect bond exists between reinforcing bars and concrete. At the level of the section, they generally require that three sets of conditions be satisfied, namely, equilibrium, compatibility of strains between the reinforcement and the matrix, and the constitutive relationship of the materials involved, that is the relationship between the strain and the stress in each material. Generally the tensile resistance of the concrete is neglected and its compressive response is modeled by a prediction equation. Numerous prediction equations for the compressive stress-strain response of plain and confined concrete can be found in the technical literature. Constitutive equations for fiber reinforced concrete are more complex especially if they are to be expressed in terms of the fiber reinforcing parameters. Examples include the case of fiber reinforced mortar in compression and SIFCON in tension [2,23,45] (see also Chapter 7 for a more detailed treatment).

14.2 Modeling of RC Beams with a SIFCON Matrix

Naaman et al. [50] described the results of a nonlinear analysis model of reinforced concrete beams using a high performance fiber reinforced cement based matrix,

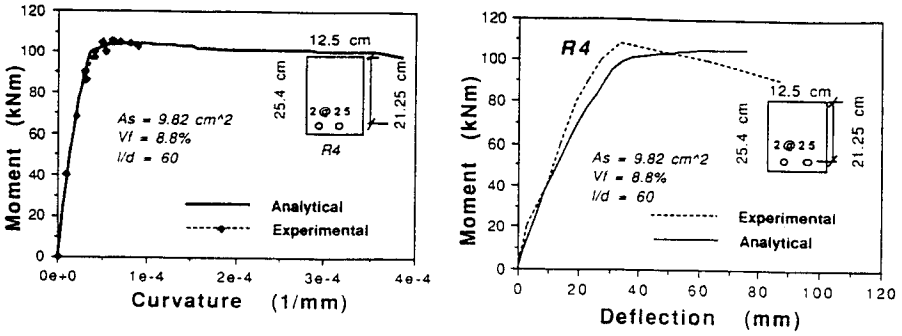

Fig. 39. Typical comparison of experimental results and analytical predictions for a) moment curvature curves, and b) moment deflection curves, of reinforced concrete beams using a SIFCON matrix.

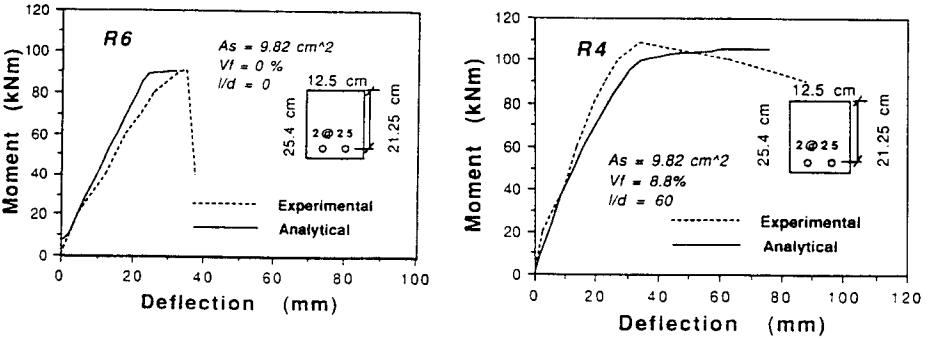

Fig. 40. Effect of fiber reinforcement on moment versus deflection curves of over-reinforced concrete beams: a) control beam, and b) beam with a SIFCON matrix.

particularly SIFCON (Slurry Infiltrated Fiber Concrete). The reason for such a combination of materials is to guarantee high structural ductility and energy absorption while maintaining high strength and otherwise over-reinforced conditions. Over-reinforced sections are defined according to the ACI Code as sections having a reinforcement ratio larger than the balanced reinforcement ratio. Two main features differentiate the model from models generally used for conventional reinforced concrete, namely: 1) the stress-strain curve of the fiber reinforced concrete matrix in compression is different from that of plain concrete, and 2) unlike the case of plain concrete, the matrix is assumed to carry a tensile load, thus, its tensile stress-strain and stress displacement relationships are predicted and used in the equilibrium equations of the section. The constitutive relationships of the FRC materials used in both compression and tension and the logical flow chart for the nonlinear analysis model are described in detail in [48a]. In all cases, the stress-strain relationships used depend on the fiber reinforcing parameters.

Analytical predictions of moment versus curvature and moment versus deflection curves were compared to experimentally observed results of reinforced concrete beams using a SIFCON (Slurry Infiltrated Fiber Concrete) matrix. Examples are shown in Figs. 39 and 40. The use of a fiber reinforced matrix in the compression zone of a reinforced concrete beam allows for otherwise over-reinforced beams to achieve significant increases in structural ductility while resisting loads close to their ultimate load. Ductility and energy ratios, normalized by the control beam without fibers, ranged from 2.47 to 3.60 and 3.28 to 5.69 respectively; that is several hundred percents in improvement. Values in the same range were also obtained from analytical predictions.

14.3 Concluding Remarks

The nonlinear analysis model described in this study was shown to predict with reasonable agreement the moment-curvature and the load deflection response of reinforced concrete beams using a SIFCON matrix. Also, the model could be used to predict the behavior of reinforced concrete beams with a plain matrix, or reinforced concrete beams with fiber reinforced cement matrices other than SIFCON, or a fiber reinforced cement matrix beam without conventional reinforcing bars. Generally the analytical model was quite optimistic at large values of deflections. This may be due to the fact that the model, in its present form, does not capture the effect of the localized failure phenomenon observed during tests in the compression zone of the concrete. An improved model could be used to undertake a parametric evaluation of the effect of different types of fiber reinforced cement matrices thus leading to optimized structural performance for a given application.

15 Concluding Remarks

The reinforced and prestressed concrete applications summarized in this Chapter, used a wide range of volume contents of fibers, from $V_f = 0.5\%$ (fiber reinforced concrete) to $V_f = 6\%$ (SIFCON). While applications with a low volume fraction of fibers did show some improvement attributed to fiber reinforcement, the improved performance could not be described as exceptional. In some cases, it was hardly noticeable. However, exceptional improvement in structural behavior was generally observed with relatively high fiber contents ($Vf \geq 2\%$). Since such fiber contents exceed the critical volume fraction of fibers needed to develop quasi-strain hardening and multiple cracking behavior (see Chapter 1), and since such behavior is specific of HPFRCCs, one can therefore conclude that the use of HPFRCCs is essential to develop superior structural behavior. This is schematically illustrated in Fig. 41 which shows that the rate of improvement in performance for $V_f > V_{fcri}$ is substantially larger than for $V_f < V_{fcri}$. Moreover, test results suggests that the use if HPFRCCs allows exploitation of the properties of conventional reinforcements to their full strain capacity. Thus, it seems

that the true success of fiber reinforced cement composites, whether in stand-alone applications or in combination with reinforced and prestressed concrete, will be appreciated only when the critical volume fraction of fibers is exceeded. Unfortunately, this opportunity has been barely explored so far and it should be viewed as the next generation of applications of fiber reinforced cement composites.

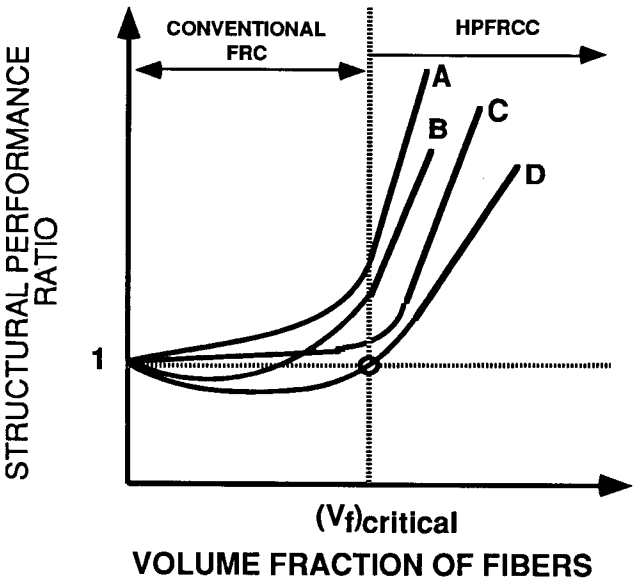

Fig. 41 Influence of HPFRCCs on structural performance

16 Acknowledgements

G. Balazs and L. Erdelyi gratefully acknowledge the financial support of the Hungarian Ministry of Education Grant 150/94.

Z. Bayasi acknowledges the financial support of Ribbon Technology Corporation for the research project on SIMCON, as well as the contribution of Mr. Jack Zeng, Ph.D. candidate in Applied Mechanics, San Diego State University.

V. Li acknowledges the contributions M. Maalej and D. Mishra for the research described using ECC.

A.E. Naaman acknowledges the contributions of former students J. Alwan, S.M. Jeong, M. Harajli, K. Soubra, R. Baccouche and S. Garcia, and is grateful to the NSF Center for Advanced Cement Based Materials for partial support.

P. Paramasivam extends his thanks to S. L. Lee, K. H. Tan, T. Y. Lim and K. Murugappan for their valuable contribution in the research program described.

17 References

1. Abdou, H.M.(1990)*Precast Construction Using Slurry Infiltrated Fiber Concrete Joints under Load Reversals,* Ph.D. Thesis, Department of Civil Eng., Univ. of Michigan, Ann Arbor.
2. Absi, E. and Naaman, A. E.(1986) Modele rheologique pour les betons de fibres, *3rd International Symposium on Fiber Reinforced Cement and Concrete*; Sheffield, UK.
3. ACI (1987) Fiber reinforced concrete properties and applications, *SP-105*, American Concrete Institute, Detroit.
4. ACI Committee 318 (1989) Building code requirement for reinforced concrete and commentary (ACI 318-89/ACI 318R-89), ACI, Detroit.
5. ACI Committee 318 (1992) Building code requirements for reinforced concrete (ACI 318R-89), *Distribution of Flexural Reinforcement in Beam and One-Way Slab*, Section R 10.6.4.; American Concrete Institute, Detroit.
6. ACI Committee 544 (1988) Measurement of properties of fiber reinforced concrete, *ACI Materials Journal*, pp. 583-593.
7. Ashour, S.A., and Wafa, F.F. (1993) Flexural behavior of high-strength fiber reinforced concrete beams, *ACI Structural Journal*, Vol. 90, No. 3, pp. 279-287.
8. Ashour, S.A., Hasanain, G.S., and Wafa, F.F.(1992) Shear behavior of high-strength fiber reinforced concrete beams, *ACI Structural Journal*, Vol. 89, No. 2, pp. 176-184.
9. Bachmann, H. (1993) *Die Massentragheit in einem Pseudo-Stoffgesetz fur Beton bei schneller Zugbeanspruchung*, Dissertation, Universität Karlsruhe.
10. Balaguru, P., and Ezeldin, A.(1987) Behavior of partially prestressed beams made with high strength fiber reinforced concrete, *Fiber Reinforced Concrete Properties and Applications*, SP-105, American Concrete Institute, Detroit, pp. 419-436.
11. Balaguru, P. (1995) *Fiber reinforced concrete: structural applications, in Fiber Reinforced Concrete: Modern Developments*, N. Banthia and S. Mindess, Editors, University of British Columbia, Vancouver, pp. 319-333.
12. Batson, G., (1985), Use of steel fibers for shear reinforcement and ductility, in proceedings of US-Sweden Joint Seminar, S.P. Shah and A. Skarendahl, Editors, Swedish Cement and Concrete Association, Stockholm, pp. 377-419.
13. Bayasi, Z.(1992) Application of carbon fiber reinforced mortar in composite slab construction, *RILEM/ACI International Workshop: High Performance Fiber Reinforced Cement Composites*, RILEM, Vol. 15, E. & FN Spon, London.
14. Bayasi, Z. and Zeng, J.(1994) Flexural behavior of slurry infiltrated mat concrete *(SIMCON)*, research report, Department of Civil Engineering, San Diego State University.
15. Brandes, K., Limberger, E. (1985) Zur Beeinflussung der Festigkeitskennwerte von Betonstahl durch die Dehngeschwindigkeit, *Beton-und Stahlbetonbau*, Heft 4, Heft 5, pp. 90-94, 128-133.
16. Burns, N.H., and Siess, C.P. (1966) Plastic hinging in reinforced concrete. *ASCE Journal of the Structural Division* 92, (ST5), pp. 45-63.
17. Chan, W.W.L. (1962) The rotation of reinforced concrete plastic hinges at ultimate load. *Magazine of Concrete Research 14* (41), pp. 63-72.
18. Chen, W.F. (1982) *Plasticity in Reinforced Concrete*, McGraw-Hill, New York.
19. Corley, W.G. (1966) Rotational capacity of reinforced concrete beams. *ASCE Journal of the Structural Division 92* (ST5), pp. 121-146.
20. Eibl, J., Bischoff, P. H., Lohrmann, G. (1992) Experiments on fibre-reinforced concrete under dynamic loading conditions, task report BRiTE./EURAM P-89-3275, Subtask 1.2, *Failure Mechanics of Fibre-Reinforce Concete ...,* 'Institut für Massivbau und Baustofftechnologie, Universität Karlsruhe.

21. Eibl, J., Lohrmann, G. (1993) Verification experiments on fibre-reinforced concrete structural elements under dynamic loading conditions, Task Report BRITE/EURAM P-89-3275, Subtask 5.3 *Failure Mechanics of Fibre-Reinforced Concrete ...*, Institut für Massivbau und Baustofftechnologies, Universität Karlsruhe.
22. Falkner, H., Kubat, B., and Droese, S. (1994) *Durchstanzversuche an Platten aus Stahlfaserbeton (Punching tests on Steel Fiber Reinforced Plates)* Bautechnik, Vol.71, No.8, pp.460-467.
23. Fanella, D. and Naaman, A.E., "Stress-strain Properties of Fiber Reinforced Mortar in Compression," *Journal of the American Concrete Institute,* Vol. 82, No. 4, July/August 1985, pp. 475-483.
24. Graig, R.J., Mahadev, S., Patel, C.C., Viteri, M., and Kartesz, C., (1984) Behavior of joints using reinforced fibrous concrete, *Proceedings of Fiber Reinforced Concrete International Symposium*, SP-81, American Concrete Institute, Detroit, Michigan.
25. Hackman, L., Farrell, M. and Dunham, O. (1992) Slurry infiltrated mat concrete (SIMCON), *Concrete Internationl*, Vol. 14, No. 12, pp. 53-56.
26. Hanecka, S., Krizma, M., Ravinger, J., and Shawkat, S. (1994) Contribution to limit state of the second group of beam subjected to moving load, *Proceedings, First Slovakian Conference on Concrete Structures*, pp.275-279.
27. Kent, D. C. and Park, R. (1971) Flexural members with confined concrete, *ASCE Journal of the Structural Division*; 1971; Vol. 97, ST-7; pp. 1969-1990.
28. Kormeling, H.A., Reinhardt, H.W., and Shah, S.P. (1987) static and fatigue properties of concrete beams reinforced with continuous bars and with fibers, *ACI Journal*, Jan.-Feb., pp.36-43.
29. Krstulovic-Opara , N., Uang, C.-M., and Haghayeghi, A. (1995) SIMCON - A novel high performance construction material for seismic repair and rehabilitation, *IABSE Symposium on Extending the Lifespan of Structures*; San Francisco, CA.
30. Krstulovic-Opara, N. and Malak, S.(1995) Tensile behavior of slurry infiltrated mat concrete (SIMCON), Under review for the *ACI Materials Journal*..
31. Krstulovic-Opara, N. and Uang, C. M.(1994) Repair and rehabilitation of non-ductile r.c. frames using high performance fiber reinforced cement composites, *NSF Earthquake Hazard Mitigation Program/BSC/ENG, Repair and Rehabilitation Program*; NSF grant # BCS-9318997.
32. Krstulovic-Opara, N., Haghayeghi, A., and Uang, C.M. (1995) The use of slurry infiltrated fiber-mat concrete (simcon) for flexural retrofit of r.c. beams, Under review for the *ACI Structural Journal*..
33. Li, V.C. (1994) Advances in Strain-Hardening Cement Based Composites, *Proceedings of Engineering Foundation Conference on Advances in Cement and Concrete*, New Hampshire, June, Ed. M.W. Grutzeck and S.L. Sarkar.
34. Lim, T. Y. (1987) *Elastic and Post Cracking Behavior of Steel Fiber Concrete*, Ph.D. Thesis, National University of Singapore.
35. Lim, T. Y., Paramasivam, P., and Lee, S. L. (1987) Analytical model for tensile behaviour of steel fibre concrete, *ACI Material Journal*, Vol. 84, No. 7, pp. 286-298.
36. Lim, T. Y., Paramasivam, P., and Lee, S. L. (1987) Shear and moment capacity of reinforced steel fibre concrete beams, *Magazine of Concrete Research*, Vol. 39, No. 140, pp. 148-160.
37. Maalej, M., and V.C. Li (1995) Introduction of strain hardening engineered cementitious composites in the design of reinforced concrete flexural members for improved durability, *ACI Structural Journal, Vol. 92, No. 2, American Concrete Institute, Detroit*..
38. Mishra, D.K., and Li, V.(1995) Performance of a ductile plastic hinge designed with an engineered cementitious composite, Submitted for publication in *ACI Structural Journal.*

39. Murugappan, K. (1993) *Shear Behavior of Reinforced and Partially Prestressed Steel Fibre Concrete Beams*, Ph.D. Thesis, National University of Singapore.
40. Murugappan, K., Paramasivam, P., and Tan, K. H. (1993) Failure envelope for steel fibre concrete under biaxial compression, *ASCE Journal of Materials in Civil Engineering*, Vol. 5, No. 4, pp. 436-446.
41. Murugappan, K., Tan, K. H. and Paramasivam, P. (1995) Finite element formulation for the analysis of reinforced fibrous concrete beams, *Finite Elements in Analysis and Design*, Vol. 18, pp. 67-74.
42. Naaman, A.E, (1992), SIFCON: tailored properties for structural performance, *High Performance Fiber Reinforced Cement Composites*, RILEM Proceedings 15, H.W. Reinhardt and A.E. Naaman, Editors, E and F.N. Spon, London.
43. Naaman, A.E., and Baccouche, M.R.(1995) Shear response of dowel reinforced SIFCON, in print *ACI Materials Journal., ACI, Detroit.*
44. Naaman, A.E., and Baccouche, M.R. (1995) Shear response of dowel reinforced SIFCON under reversed cyclic loading, to be submitted, *ACI Structureal Journal .*
45. Naaman, A. E. and Homrich, J. R.(1989) Tensile stress-strain properties of SIFCON, *ACI Materials Journal*; Vol. 86, No.3, May-June 1989, pp.244-251.
46. Naaman, A.E, "Ductility Implications of Prestressed and Partially Prestressed Concrete Structures Using Fiber Reinforced Plastic Reinforcements," FIP Symposium 93, Modern Prestressing Techniques and their Applications, Kyoto, Japan, October 1993.
47. Naaman A.E., and Jeong S.M.(1995) Structural ductility of concrete beams prestressted with FRP tendons, in press *FIP 2nd International Symposium on FRP Reinforcements for Concrete Structures*, Ghent, Belgium.
48. Naaman, A. E. and Jeong, S. M. (1994) Investigation of beams partially prestressed with carbon fiber composite tendons, *Proceedings of FIP-XIIth International Congress, Washington*, pp B56-B61.
49. Naaman, A.E., Reinhardt, H.W., and Fritz, C.(1992) Reinforced concrete beams with a SIFCON matrix, *ACI Materials Journal,* V. 89, No. 1, pp. 79-88.
50. Naaman, A. E., Reinhardt, H. W., Fritz, C., and Alwan J.(1993) Non-linear analysis of RC beams using SIFCON matrix, *Materials and Structures*; Vol. 26; pp. 522 - 531.
51. Naaman, A.E., Harajli, M.H. and Wight, J.K., "Analysis of Ductility in Partially Prestressed Concrete Flexural Members," *PCI Journal,* Vol. 31, No. 3, May-June 1986, pp. 64-87. See also closure to discussion in PCI Journal, Vol. 32, No.1, Jan.-Feb. 1987, pp. 142-145.
52. Naaman, A.E., Wight, J.K., and Abdou, H.(1987) SIFCON connections for seismic resistant frames, *Concrete International,* Vol.9, No. 11, pp. 34-39.
53. Narayanan, R., and Darwish, I.Y.S. (1987) Use of steel fibers as shear reinforcement, *ACI Structural Journal*, pp.216-227.
54. Nielson, M.P. (1984) *Limit Analysis and Concrete Plasticity,* Prentice-Hall, New Jersey.
55. Paramasivam, P., Tan, K. H., and Murugappan, K. (1995) Finite element analysis of partially prestressed steel fibre concrete beams in shear, Accepted for publication, *ACBM Journal.*
56. Porter, M.(1984) Proposed design criteria for composite steel deck slabs, *Proceedings, U.S./Japan Joint Seminar*, American Society of Civil Engineers, pp. 28-41.
57. Quassem, N., and Hassoun, N. (1993) *Effect of steel fibers on the plastic rotation ymposium 1978*, Constuction Press, Lancester, UK.
58. Reinhardt, H.W., and Naaman, A.E. editors (1992) High performance fiber reinforced cement composites, *Proceedings of the Rilem/ACI Workshop*, Mainz, June 23-26, 1991, RILEM, Vol. 15, E. & FN Spon, London, 565 pages.
59. RILEM (1978) Testing and test methods of fiber cement composites, *Proceedings of the RILEM Symposium 1978*, Construction Press, lancester, UK.

60. Romualdi, J.P., and Batson, R.G. (1963) Behavior of reinforced concrete beams with closely spaced reinforcement, *ACI Journal*, Vol.60, No.6, pp.775-790.
61. Romualdi, J.P., and Mandel, J.A. (1964) Tensile strength of concrete affected by uniformly distributed and closely spaced short lengths of wire reinforcement, *ACI Journal*, Vol.61, No.6, pp.657-671.
62. Sargin, M.(1971) *Stress-strain relationship for Concrete and the Analysis of Structural Concrete Sections*; Study No. 4; Solid Mechanics Division, University of Waterloo, Ontario, Canada.
63. Soubra, K., Wight, J.K., and Naaman, A.E.(1993) Cyclic response of cast-in-place connections in precast beam-column subassemblages, *ACI Structural Journal*, Vol. 90, No. 3, pp. 316-323.
64. Soubra, K., Wight, J.K., and Naaman, A.E.(1991) Fiber reinforced concrete joints for precast construction in seismic areas, *ACI Structural Journal,* Vol. 88, No. 2, pp. 214-221.
65. Swamy, R.N., and Bahia, H.M., (1985), The effectiveness of steel fibers as shear reinforcement, Concrete International, Vol. 7, No. 3.
66. Tan, K. H, Murugappan, K. and Paramasivam, P. (1993) Shear behaviour of reinforced steel fibre concrete beams, *ACI Structural Journal,* Vol. 90, No. 1, pp. 3-11.
67. Tan, K. H., Murugappan, K., and Paramasivam, P. (1994) Constitutive relations for steel fibre concrete under biaxial compression, *Cement and Concrete Composites*, Vol. 16, pp. 9-14.
68. Tan, K.H., Murugappan, K., and Paramasivam, P., (1995) Steel fibers as shear reinforcement in partially prestressed beams, accepted for publication, *ACI Structural Journal*.
69. Tassi G., and ErdElyi L., (1984) The time-dependent change of the transmission length in prestressed pre-tensioned members, *Proceedings RILEM-ACI Symposium Long Term Observation of Concrete Structures,* pp.21-29.
70. Tsukamoto, M.(1990) Tightness of fiber concrete, *Darmstadt Concrete, Annual Journal on Concrete and Concrete Structures*, V. 5, pp. 215-225.
71. Wafa, F.F, and Ashour, S.A.(1992) Mechanical properties of high-strength fiber reinforced concrete beams, *ACI Materials Journal,* Vol. 89, No. 3, pp. 449-455.
72. Wafa, F.F., Hasnat, A., and Tarabolsi, O.F.(1992) Prestressed fiber reinforced concrete beams subjected to torsion, *ACI Structural Journal,* Vol. 89, No. 3, pp. 272-283.
73. Balazs, G. and Erdelyi, L.(1995) *Behavior of prestressed SFRC under tension release*, full contribution to this Chapter, 15 pages.
74. Hassoun, N. , 1995, Contribution to this chapter.
75. Paramasivam, P., 1995, Contribution to this chapter.